UNCLASSIFIED

AD **436404**

DEFENSE DOCUMENTATION CENTER

FOR

SCIENTIFIC AND TECHNICAL INFORMATION

CAMERON STATION, ALEXANDRIA, VIRGINIA

UNCLASSIFIED

64-12

DDC
APR 23 1964

HYDRONAUTICS, incorporated
research in hydrodynamics

HYDRONAUTICS, Incorporated

AN ANALYTICAL STUDY OF THE HYDRODYNAMIC PERFORMANCE OF WINGED, HIGH-DENSITY TORPEDOES

By

C. F. Chen

October 1963

HYDRONAUTICS, Incorporated

TABLE OF CONTENTS

HYDRONAUTICS, Incorporated

LIST OF FIGURES

HYDRONAUTICS, Incorporated

HYDRONAUTICS, Incorporated

NOTATION

A aspect ratio of wing $= \dfrac{4(b - \sqrt{1 - \gamma^2} R_b)^2}{S_w}$

A_t aspect ratio of the ring tail $= \dfrac{D_m}{C_{rt}}$

B buoyancy force

b distance from center of torpedo to tip of wing

$\ell.c.$ specific fuel consumption: lb-fuel/HP-Hr.

C chord of wing

C_A total drag coefficient based on the wetted surface area of a body of revolution

C_D drag coefficient

C_{D_o} together with K defines the profile drag of the wing section

$\overline{C}_D$ drag coefficient based on $(V_w)^{\frac{2}{3}}$

C_f friction coefficient

C_L total lift coefficient based on exposed wing area

C_{L_w} lift coefficient developed on the wing

$C_{L\alpha}$ lift curve slope

C_{pr} prismatic coefficient $= \dfrac{V_b}{\frac{\pi}{4} D_m^2 \, \ell}$

C_{rt} chord of ring tail

C_s surface coefficient $= \dfrac{S_b}{\pi \, D_m \, \ell}$

HYDRONAUTICS, Incorporated

$\overline{C}_w$ weight coefficient $= \dfrac{W}{qV_w^{\frac{2}{3}}}$

D   total drag

D_m maximum diameter of torpedo

$\overline{D}_m$ $= D_m/(V_w)^{\frac{1}{3}}$

$G(\gamma, R_b')$ algebraic function defined by Equation [30]

I   moment of inertia

K, K_1 constants

L   lift

ℓ length of torpedo

ℓ_c length of central cylindrical portion of the torpedo

ℓ_t distance from the c.g. of torpedo to the c.p. of ring tail

M   pitching moment

q   dynamic pressure $= \frac{1}{2}\rho_w U^2$

R   buoyancy ratio $= \dfrac{B}{W}$

R_b radius of body

R_b' $= R_b/b$

Re_ℓ Reynolds number based on ℓ

Re_t Reynolds number based on C_{rt}

Re_v Reynolds number based on $V_w^{\frac{1}{3}}$

S   range in miles

S_b surface area of body

HYDRONAUTICS, Incorporated

S_w wing planform area

$S_v{}'$ ratio of the wetted area of the supporting vanes to area of ring tail

S_t surface area of ring tail

s maximum allowable stress

s' $= s V_w^{\frac{2}{3}} W$

T thrust

t thickness ratio $= D_m/\ell$

U uniform stream velocity

V_b volume of the torpedo

V_w volume of water whose weight is W, $V_w = \dfrac{W}{\rho_w g}$

W total weight of torpedo

W_F total fuel weight

$\bar{x}$ distance from the nose of a body of revolution to the transition point

y_{max} distance from vertical axis to the outermost fiber

$\bar{z}$ nondimensional sectional modulus $= \dfrac{I}{y_{max} C^3}$

α angle of attack

γ γR_b is the distance from the centerline of the torpedo to a horizontally mounted wing.

η propulsive efficiency

HYDRONAUTICS, Incorporated

θ	climbing angle
ρ_b	density of body
ρ_w	density of water

subscripts

b	body
r	wing root
t	tail, or wing tip
w	wing

HYDRONAUTICS, Incorporated

ABSTRACT

The hydrodynamic performance of winged torpedoes has been investigated. It is assumed that the wing is mounted such that its center of pressure coincides with the center of gravity of the body, and that a ring-tail stabilizer is used. The resulting overall lift-drag ratios are presented as functions of the buoyancy-weight ratio. The advantages of the winged torpedoes over those with neutral buoyancy become more pronounced as the nondimensional parameter $\overline{C}_W$ becomes smaller, and as the buoyancy-weight ratio decreases. $\overline{C}_W$ is defined as $W \left/ \frac{1}{2}\rho_W U^2 (V_W)^{\frac{2}{3}} \right.$, where W is the weight; $\frac{1}{2}\rho_W U^2$, the free stream dynamic pressure; and V_W is the volume of water with weight, W. Parametric studies of the lift-drag ratio obtainable have been carried out with respect to the following quantities: the Reynolds number based on $(V_W)^{\frac{1}{3}}$, the nondimensional strength factor of the wing material, and the maximum allowable diameter. In conclusion, the ranges obtainable for the ascending, level, and descending flights are calculated. It is found that if the fuel weight is assumed to be always one-half of the displacement, winged torpedoes have longer ranges than those with neutral buoyancy only for descending missions. If the fuel weight, however, is assumed to be one-half of the total weight, the winged torpedo has longer ranges for all missions except steep ascending ones.

INTRODUCTION

Up to now, torpedoes have been generally designed with neutral buoyancy. If one departs from this concept and considers a winged torpedo, for which part of the weight is carried by the dynamic lift generated on the wings, a more efficient torpedo, depending on the design weight and speed, may be evolved. In this report, a preliminary investigation has been made on the overall lift-drag ratio obtainable, the size of the wing needed, and the range of travel for winged torpedoes at different values of buoyancy to weight ratios.

In the calculations, it is assumed that the wing is mounted such that its center of pressure coincides in axial position with that of the center of gravity of the torpedo. The assumption simplifies the tail selection for which considerations of stability must be made. We also assume that a ring tail is used to provide the required stability. Two types of bodies are considered: one is the optimum body for a given volume; the other is a diameter-limited body (i.e., limited to the maximum allowable size for use in existing torpedo tubes). In the following, the methods by which the component drags and the range are calculated are developed and the results of such calculations are presented and discussed.

METHODS OF CALCULATION

A. Drag

Let the weight of the torpedo be W; let the drag due to the body, tail, and wing be denoted by D_b, D_t, and D_w respectively. The overall lift to drag ratio is

$$\frac{W}{D} = \frac{W}{D_b + D_t + D_w} \; . \tag{1}$$

The buoyancy to weight ratio, or in other words the ratio of the density of water ρ_w, to that of the torpedo, ρ_b, is denoted by R,

$$R = \frac{B}{W} = \frac{V_b \rho_w g}{V_w \rho_w g} = \frac{V_b}{V_w} \; ; \; R = \frac{B}{W} = \frac{V_b \rho_w g}{V_b \rho_b g} = \frac{\rho_w}{\rho_b} \; , \tag{2}$$

where B denotes the total buoyancy force. To normalize the forces, we use the dynamic pressure of the uniform stream, $\frac{1}{2}\rho_w U^2$, and $(V_w)^{\frac{2}{3}}$, where V_w is the volume of water whose weight is W:

$$V_w = \frac{W}{\rho_w g} \; . \tag{3}$$

For a constant weight and constant forward speed U, the normalizing force, $\frac{1}{2}\rho_w U^2 (V_w)^{\frac{2}{3}}$, is constant. Let

$$\overline{C}_w \equiv \frac{W}{\frac{1}{2}\rho_w U^2 (V_w)^{\frac{2}{3}}} \; ; \tag{4}$$

It then follows that

$$\frac{W}{D} = \frac{\overline{C}_w}{\overline{C}_{d_b} + \overline{C}_{d_t} + \overline{C}_{d_w}} \; . \tag{5}$$

HYDRONAUTICS, Incorporated

In the following, we examine each drag component separately.

(1) Body Drag

In the total drag of the body, (skin friction plus form drag), we use the results of Young (Reference 1). Young's calculation of total drag coefficients based on wetted surface area, C_A, are presented in graphical form. To facilitate computation by the IBM 1620 digital computer, the process of curve-fitting has been carried out to give the following formula:

$$C_A = 10^{-2} \times [.035(g - \log_{10} Re_\ell)^2 + .215 - .24 \, \overline{x}/\ell - (.2 - t)Y].$$
[6]

$$Y = \begin{cases} .78 - .28(\log_{10} Re_\ell - 6) + .12(\log Re_\ell - 7)^2 & t > .2, \\ \\ .37 - .12(\log_{10} Re_\ell - 6) + .04(\log Re_\ell - 7)^2 & t < .2, \end{cases}$$
[7]

in which Re_ℓ denotes the Reynolds number based on body length ℓ; $\overline{x}$, distance from the nose to the transition point; t, the thickness ratio. In the optimum body, t = 0.2, and the expression for C_A is considerably simplified.

Since the comparisons will be carried out at constant speed and weight, the Reynolds number based on $V_w^{\frac{1}{3}}$ is considered known:

$$Re_V = \frac{UV_w^{\frac{1}{3}}}{\nu} .$$
[8]

To calculate Re_ℓ from Re_V, we first define the (logitudinal) prismatic coefficient C_{pr} as

$$C_{pr} \equiv \frac{V_b}{\frac{\pi}{4} D_m^2 \ell} , \qquad [9]$$

where V_b is the volume and D_m the maximum diameter of the body. By the definitions of the buoyancy — weight ratio and the thickness ratio, we obtain from [9]

$$V_w = \frac{\pi}{4R} C_{pr} t^2 \ell^3 . \qquad [10]$$

The Reynolds number based on body length is then

$$Re_\ell = \frac{Re_v}{\left(\frac{\pi}{4R} C_{pr} t^2\right)^{\frac{1}{3}}} . \qquad [11]$$

To obtain $\overline{C}_{D_b}$, we define a surface coefficient C_s

$$C_s \equiv \frac{S_b}{\pi D_m \ell} , \qquad [12]$$

where S_b is the wetted area of the body. By simple algebra, we obtain

$$\overline{C}_{D_b} = C_A C_s \left[\frac{16\pi R^2}{C_{pr}^2 t}\right]^{\frac{1}{3}} , \qquad [13]$$

where C_A is obtainable from Equations [6] and [7].

For definiteness, we shall consider that the optimum body is a spheroid of thickness ratio 0.2, and the diameter-limited body

HYDRONAUTICS, Incorporated

is made up of a central cylindrical section of length ℓ_c and two semi-spheroidal noses. In such a composite body, the prismatic and surface coefficients are easily computed to be

$$C_{pr} = \frac{2 + \ell_c/\ell}{3} \ . \qquad [14]$$

and

$$C_s = \frac{\ell_c}{\ell} + \tfrac{1}{2} \left[(1 - \frac{\ell_c}{\ell} (1 - t^2)^{-\frac{1}{2}} \sin^{-1}(1 - t^2)^{\frac{1}{2}} + t \right]. \qquad [15]$$

For a spheroid, $\ell_c/\ell = 0$,

$$C_{pr} = 2/3 \ , \qquad [16a]$$

$$C_s = \tfrac{1}{2} \left[(1 - t^2)^{-\frac{1}{2}} \sin^{-1}(1 - t^2)^{\frac{1}{2}} + t \right] \ . \qquad [16b]$$

Let $\overline{D}_m = D_m V_w^{-\frac{1}{3}}$ be the nondimensional maximum diameter. By the definition of the prismatic coefficient, we can write the thickness ratio t as

$$t = \frac{\pi}{12} (2 + \ell_c/\ell) \overline{D}_m^3 \ . \qquad [17]$$

The volume of the body is

$$V_b = \frac{\pi D_m^2}{12} \ \ell (2 + \ell_c/\ell)$$

$$= \frac{\pi}{12} \ \overline{D}_m^2 \ell^3 \left(\frac{\pi}{4R} C_{pr} t^2 \right)^{\frac{2}{3}} \left(2 + \ell_c/\ell \right) \ . \qquad [18]$$

In the optimum body, $t = 0.2$, and $C_{pr} = 2/3$. C_s may be calculated according to [16b]. Equation [13] together with [6] gives the required value of $\overline{C}_{D_b}$. For a diameter-limited body, ℓ_c/ℓ and $\overline{D}_m$ must be specified. From these values, C_{pr} and t are calculated according to [14] and [17] respectively. C_s may be obtained by [15], together with the value of C_A obtainable from [6] and [7], and $\overline{C}_{D_b}$ can again be calculated.

(2) Tail Drag

We assume that the position of the wing is such that it does not contribute to the moment when the entire configuration is pitched. According to experience, the static restoring moment generated by the tail is usually some fraction of the static destabilizing moment generated by the body. The configuration must be dynamically stable. We design the tail such that

$$M_t = K_1 M_b, \quad K_1 > 0, \tag{19}$$

where M_t and M_b denote moments due to the tail and the body respectively; K_1 is a constant. $K_1 > 0$ implies that the moments are opposite in sense. By slender body theory, at a pitch angle α

$$M_b = \rho_w U^2 V_b \alpha . \tag{20}$$

The moment generated by the tail may be written in terms of the lift curve slope of the tail, $C_{L\alpha t}$, the dynamic pressure q, the

HYDRONAUTICS, Incorporated

tail surface area, S_t, and the distance from the c.g. of the body to the tail center of pressure, ℓ_t:

$$M_t = C_{Lat} q S_t \ell_t \alpha .$$ [21]

Equation [19] gives then

$$C_{Lat} = \frac{\pi K_1 C_{pr} t^2 \ell^3}{2 S_t \ell_t} .$$ [22]

For a ring tail

$$\begin{cases} S_t = \pi D_m C_{rt} , \\[2ex] A_t = \dfrac{D_m}{C_{rt}} , \end{cases}$$ [23]

in which C_{rt} is the chord of the ring tail. The diameter of the ring tail is taken as the maximum diameter of the body. Using the definition S_t and A_t, [22] becomes

$$\frac{C_{Lat}}{A_t} = \tfrac{1}{2} K_1 C_{pr} \, \ell/\ell_t .$$ [24]

Weissinger (Reference 2) gives the effectiveness of a ring wing approximately as

$$\frac{A_t}{C_{Lat}} \simeq \tfrac{1}{2} + \frac{1}{\pi} \left(A_t + \tan^{-1} \frac{1.2}{A_t} \right) .$$ [25]

HYDRONAUTICS, Incorporated

Solving [24] and [25] simultaneously, we obtain the aspect
ratio of the tail A_t, thence

$$\left(A_t + \tan^{-1} \frac{1.2}{A_t} \right) = \frac{\pi}{2} \left(K_1 C_{pr} \, \ell/\ell_t - 1 \right) . \qquad [26]$$

To determine the frictional drag, we calculate the Reynolds
number of the tail

$$Re_t = \frac{UC_{rt}}{\nu} = \frac{t}{A_t} Re_\ell . \qquad [27]$$

The drag of the tail non-dimensionalized with respect to $qV_w^{\frac{2}{3}}$
is

$$\overline{C}_{D_t} = C_f \left\{ \frac{128\pi t^2 R^2}{C_{pr}^2} \right\}^{\frac{1}{3}} \left(\frac{1 + S_v{}'}{A_t} \right) , \qquad [28]$$

where $S_v{}'$ is ratio of the wetted surface area of the supporting
vanes to that of the tail, and C_f is the friction coefficient.

(3) Wing Drag.

The drag of the wing can only be determined after the wing
has been sized. Preliminary considerations show that the wings
may be of small aspect ratio, say near 1, and of small span.
The interference effects between the wing and the body must now be
considered.

At the design condition, the body is considered to be
at zero angle of attack, while the wing is set so that the desired

amount of lift is developed. Lawrence and Flax (Reference 3) have considered the interference lift generated on an infinite circular cylinder due to a finite lifting line of arbitrary lift distribution mounted therein. The problem is solved in the Trefftz plane by the use of Green's theorem. The interference lift generated on the body can be obtained by an integration along the wing of the product of the lift distribution and the velocity component normal to the wing due to a vertical translation of the cylinder. In their paper, Lawrence and Flax (Reference 3) calculated the interference lift on the cylinder due to a constant, elliptic, and optimum lift distribution on a centrally-mounted, horizontal lifting line. The results do not differ appreciably. Furthermore, they have shown that the lift on the body subsides in about two diameters in either direction from the lifting line; the idealization of an infinite cylinder for the body is thus not without justification. In the present case, we have calculated the total lift of the wing-body system (lift on wing + interference lift on body) for a horizontal lifting line of constant lift distribution, whose tip to tip distance is 2b, mounted γR_b above the center of the cylinder of radius R_b. Defining the lift coefficient with respect to the wing area S_w, we obtain

$$C_L = \frac{L}{q S_w} = C_{L_w} G(\gamma, R_b') , \qquad [29]$$

$$G(\gamma, R_b') = \frac{1 - (1 - \gamma^2) R_b'^2}{[1 - (1 - \gamma^2)^{\frac{1}{2}} R_b'](1 + \gamma^2 R_b'^2)} , \quad [30]$$

where $R_b' = R_b/b$. For wings of large span, $R_b' \rightarrow 0$, $G(\gamma, 0) = 1$, then

$$C_L \cong C_{L_W} \; .$$

The function G is shown in Figure 1 for different values of γ. It is seen that centrally mounted wings are the most efficient in producing the interference lift on the body. However, for the present application, the wings will necessarily be stored within the body prior to and during the launch and a centrally mounted wing may not be feasible.

Before we select the wing which will carry the required lift while incurring the least amount of drag for our present winged torpedo system, it is instructive to consider briefly the optimum design of an isolated wing. In general, the drag coefficient of a wing may be written as

$$C_D = C_{D_O} + KC_L^2 + \frac{C_L^2}{\pi A} (1 + \delta) \; , \qquad [31]$$

in which the first two terms are the profile drag of the wing section and the last term is the induced drag; δ is the factor introduced to take into account that the loading may not be elliptical. Dividing [13] through by C_L, and finding the minimum C_D/C_L we obtain

$$\left(\frac{C_D}{C_L} \right)_{min} = 2 \; C_{D_O}^{\frac{1}{2}} \left(K + \frac{1 + \delta}{\pi A} \right)^{\frac{1}{2}} \; , \qquad [32]$$

HYDRONAUTICS, Incorporated

in which the optimizing components are

$$\left(c_L\right)_{opt} = \left(\frac{c_{D_o}}{K + \frac{1 + \delta}{\pi A}}\right)^{\frac{1}{2}} \tag{33}$$

and

$$\left(c_D\right)_{opt} = 2\, c_{D_o} \,. \tag{34}$$

It is seen that the larger the aspect ratio, the smaller the resulting drag for the same lift. However, the aspect ratio is limited by the bending stress allowable at the mid-span. For elliptic loading, the bending moment at the mid-span is

$$\frac{2}{3\pi}\, Lb = \frac{I_s}{y_{max}} \,, \tag{35}$$

in which I is the moment of inertia and y_{max} is the distance from the neutral axis to the outermost fiber, and s is the tensile stress at the outermost fiber. Rewriting and transposing, assuming a rectangular wing we obtain

$$c_L A^2 = 3\pi\, \bar{z}\, \frac{s}{q} \,, \tag{36}$$

in which $\bar{z}$ is the nondimensional sectional modulus

$$\bar{z} = \frac{I}{y_{max} c^3} \,. \tag{37}$$

When the working stress of the wing material is given, Equations [33] and [36] determine the optimum aspect ratio and C_L.

Returning now to the winged torpedo, we follow the same procedure as above with the added complications that: (a) the profile drag is only found on the exposed wing, while the induced drag may be calculated according to the full span 2b, (b) the maximum bending stress is at the wing-body juncture, (c) the lift developed by the wing is some fraction of the total lift required depending upon the position of the wing with respect to the center of the body, and (d) we allow the wing to be tapered. With these considerations, the counterpart of [33] is

$$C_{L_w} = \frac{C_{D_o}^{\frac{1}{2}}}{\left\{ K + \frac{1 + \delta}{\pi A} G(\gamma, R_b') [1 - (1 - \gamma^2)^{\frac{1}{2}} R_b'] \right\}^{\frac{1}{2}}} \qquad [38]$$

and that of [36] is

$$C_{L_w} A^2 = \frac{24\pi}{(1 + C_t/C_r)^3} \, \bar{z}_r \, \frac{s}{q} \, , \qquad [39]$$

where C_t and C_r denote the chord at the tip and the root respectively, and $\bar{z}_r$ is the nondimensional sectional modulus of the root section. The aspect ratio A is that of the exposed wing. Let now the working stress be nondimensionalized with respect to $WV_w^{-\frac{2}{3}}$, and writing it as s', [39] becomes

$$C_{L_w} A^2 = \frac{24\pi}{(1 + C_t/C_r)^3} \ \bar{z}_r \ s' \ \bar{C}_w \ . \qquad [40]$$

Because of the added variable R_b', another equation is needed.
This is obtained by considering the relation between C_{L_w} and W:

$$C_{L_w} = \frac{W(1 - R)}{G(\gamma, R_b')q \ S_w}$$

$$) = \frac{\bar{C}_w(1 - R)}{G(\gamma, R_b')} \ \frac{V_w^{\frac{2}{3}}}{S_w} \ . \qquad [41]$$

Rewriting the wing area S_w in terms of aspect ratio and V_w
according to [10], we obtain

$$C_{L_w} = \frac{\bar{C}_w(1 - R)}{G(\gamma, R_b')} \ \frac{R_b'^2 \ (C_{pr} \ \frac{\pi}{4R})^{\frac{2}{3}}}{[1 - (1 - \gamma^2)^{\frac{1}{2}} R_b']^2} \ A \ . \qquad [42]$$

Equations [38], [39], and [42] determine C_{L_w}, A, and R_b' for
given values of γ, C_{pr}, t, C_t/C_r, $\bar{z}_r$, $\bar{C}_w$, R, δ, K, and C_{D_o}.
Now it is an easy matter to determine the drag contribution
due to the wing:

$$\bar{C}_{D_w} = \frac{2C_{D_o} S_w}{q \ V_w^{\frac{2}{3}}} \ . \qquad [43]$$

HYDRONAUTICS, Incorporated

By the use of [41], we obtain

$$\overline{C}_{D_W} = \frac{2C_{D_O}}{q} \frac{\overline{C}_W(1-R)}{C_{L_W} G(\gamma, R_b')} .$$ [44]

These expressions have been programmed for computation on the IBM 1620 Computer for the following values of the constants:

$$K = .012$$
$$C_{D_O} = .009$$
$$\delta = 0$$
$$C_t/C_r = .5$$
$$\ell_c/\ell = .5$$
$$\overline{x} = 0$$
$$\gamma = 0.7$$
$$K_1 = 0.7$$
$$S_v' = .5$$

The value of K and C_{D_O} determine the profile drag of the wing which should be a function of the Reynolds number. In the present calculation, they are assumed to be constant. Since the wing drag is usually one order of magnitude smaller than the body drag, the simplification should not incur too much of an error. In order to select a suitable range of values for $\overline{C}_W$, we have

calculated $\overline{C}_W$ for a 3000 pound and 6000 pound torpedo with forward

speeds of 10 to 100 knots. The results are shown in Figure 2. It is seen that the value of $\overline{C}_w$ ranges from 0.01 (at about 100 knots) to 1 (at about 10 knots). The difference in the weight of the torpedo has no appreciable effect on the value of $\overline{C}_w$, since it is proportional to $W^{\frac{1}{3}}$.

The computation scheme is as follows: For assumed values of Re_v, the product $s'\,\overline{z}$, and $\overline{D}_m$, the value of $\overline{C}_w$ is systematically varied. For each value of $\overline{C}_w$, the buoyancy ratio R is varied from 0.2 to 1.0. In each of these cases, the component drags, the overall lift-to-drag ratio W/D, the lift coefficient C_{L_w}, aspect ratio A and the radius-span ratio R_b' are calculated for both the optimum body (t = 0.2 spheroid) and the diameter limited body. The following six cases have been computed:

	Re_v	$s'\,\overline{z}$	$\overline{D}_m$
1	1.2×10^8	0.7	.481
2	6×10^6	0.7	.481
3	6×10^6	33.0	.383
4	6×10^6	33.0	.481
5	4×10^7	.7	-
6	8×10^7	.7	-

In cases 5 and 6, only optimum bodies are calculated. The results from cases 1 and 2, together with 5 and 6 give the Reynolds number effect; cases 2 and 4 give the effect of $s'\,\overline{z}$; cases 3 and 4 give the effect of $\overline{D}_m$.

HYDRONAUTICS, Incorporated

B. Range

Let the torpedo be ascending at an angle θ with respect
to the horizontal. When in uniform motion, the thrust balances
the drag and the component of the effective weight, i.e., weight
less buoyancy, in the direction of flight:

$$T = (W - B) \sin \theta + D. \qquad [45]$$

Let $l.c.$ be the specific fuel consumption in weight of fuel per
unit power output of the engine, η be the propulsive efficiency.
The rate at which weight of fuel, W_F, is being spent is then

$$\frac{dW_F}{dt} = \frac{l.c. \, TU}{\eta} \quad . \qquad [46]$$

Rewriting [46] and using [45], we obtain

$$\frac{l.c.}{\eta} \, Udt = \frac{dW_F}{(W - B) \sin \theta + D} \quad . \qquad [47]$$

Assuming now both the specific fuel consumption, $l.c.$, and the
propulsive efficiency, η, stay essentially constant, the left-hand
side integrates out to be $l.c. \, S/\eta$, where S is the range. In
torpedo applications, the weight of the torpedo is kept constant
by using water to displace the fuel. If the density of the
stored fuel is comparable to that of water, the buoyancy B stays
constant; the total drag of the torpedo D is also a constant.

HYDRONAUTICS, Incorporated

-18-

Then [47] gives

$$\frac{\ell.c.}{\eta} \, S = \frac{W_F}{W(1-R) \, \sin \theta + D} \, , \qquad [48]$$

in which W_F is the total fuel weight. Writing in terms of the lift-drag-ratio, [48] becomes

$$\frac{\ell.c.}{\eta} \, S = \frac{W_F}{W} \, \frac{W/D}{\frac{W}{D}(1-R)\sin \theta + 1} \, . \qquad [49]$$

It is seen from [49] that if θ is the glide angle

$$\theta = - \sin^{-1} \frac{1}{\frac{W}{D}(1-R)} \, , \qquad [50]$$

and the torpedo will travel on indefinitely without expending any fuel.

To facilitate calculation, we use the following units for the quantities on the left of Equation [49]:

$$\ell.c. = \text{lb fuel/horsepower - hour,}$$
$$S \; = \text{range in miles.}$$

Then the range expression becomes

$$\frac{\ell.c.S}{\eta} = 375 \, \frac{W_F}{W} \, \frac{W/D}{\frac{W}{D}(1-R)\sin \theta + 1} \text{ miles-lb fuel/horsepower-hour.}$$

$$[51]$$

Calculations of the range factor $\ell.c.$ S/q have been made for the optimum body configuration at $\mathrm{Re}_v = 1.2 \times 10^8$ and s' $\overline{z}$ = 0.7 (corresponding to case 1). Two different assumptions have been made on the fuel weight: in the first case we assume that the fuel weight equals one-half of the displacement; in the second case, we assume that it equals one-half of the total weight.

RESULTS AND DISCUSSIONS

A. Lift-Drag Ratio

In Figure 3, we have presented the results of case 1; the lift-drag ratio is shown as a function of the buoyancy ratio with $\overline{C}_w$ as a parameter. The results for the torpedo with the optimum body is shown in solid lines while that for the diameter-limited body is shown in dash lines. The lift-drag ratio, W/D, is plotted along a logarithmic scale, since in this way, irrespective of the values of W/D at R=1, $(W/D)_1$, an x-fold increase therefrom will appear a constant linear distance (log x) above $(W/D)_1$. The steeper the curves of W/D, the larger the relative increase of W/D. The smaller the $\overline{C}_w$, the larger the effect of decreasing the buoyancy ratio on the improvement of W/D. The effect of limiting the body diameter is always detrimental to the value of W/D obtainable. In Figure 4, we have shown the drag breakdown for this case of $\overline{C}_w$, which is quite typical. It is seen that a major portion of the drag is due to the body. If by some means the drag of the body can be reduced (e.g., by boundary layer suction, by the use of cavity running torpedoes or through the use of stabilizing additives), the resulting W/D can be further increased.

In Figures 5 and 6, only the results from the optimum body for cases 2 and 3 are presented. In Figure 5, intermediate values of $\overline{C}_W$ = 0.75 and 0.5 have been calculated and presented.

It is seen that for $\overline{C}_W$ greater than 0.5, there is no advantage to be gained by using wings. However at the lower values of $\overline{C}_W$, say, 0.01 ($\approx$ 3000 pound torpedo at 90 knots, c.f. Figure 2), the value of W/D at R = .2 is nearly 3 times that at R = 1.0.

Cross-comparing Figures 5 and 6, it is seen that the effect of s' $\overline{z}$ on the resulting W/D is quite small. The larger value of s' $\overline{z}$ permits the use of higher aspect-ratio wings with concomitant savings in the wing drag. However, the drag due to the wing constitutes only a small portion of the total drag, as shown in Figure 4, and the savings show up significantly only for $\overline{C}_W \geq$ .1, and only at small R's.

In Figure 7, the effect of the maximum allowable diameter is shown. The smaller diameter body, having a surface area larger than that of the bigger diameter body for enclosing the same volume, incurs larger drag. This explains the difference in W/D at R=1. However, the improvement on W/D can be made larger for the smaller diameter body.

Figures 8 and 9 refer to cases 5 and 6. Cross-comparing these two figures with Figures 3 and 5, we obtain the effect of the Reynolds number, Re_v. The W/D obtainable are smaller for smaller Re_v. However, as we shall see in Figure 13, the Reynolds number has little effect on the improvements attainable on W/D.

HYDRONAUTICS, Incorporated

In Figures 10 through 13, we have shown the improvements on W/D attainable as a function of $\overline{C}_w$. We define the nondimensional increase in lift-drag ratio $\Delta(W/D)$ as

$$\Delta(W/D) \equiv \frac{W/D)_{R=.2} - W/D)_{R=1}}{W/D)_{R=1}} \qquad [52]$$

When $\Delta(W/D) = 1$, the lift-drag ratio at buoyancy ratio $R = 0.2$ is twice that at $R = 1$. In Figure 10, $\Delta(W/D)$ is plotted vs. logarithm of $\overline{C}_w$ for case 1. It is seen that for $\overline{C}_w \geq 0.4$, the winged torpedo is less efficient than the neutrally buoyant one. At low values of $\overline{C}_w$, the torpedo which consists of the diameter-limited body is not as efficient as that with the optimum body. In the same Figure, the aspect ratio of the wing A_w and the span-diameter ratio, or equivalently half-span-radius ratio, b/R_b, for the optimum-body torpedo at $R = .2$ are also shown. It is seen that at $\overline{C}_w \approx .01$, the wing span as well as the aspect ratio are quite small; $A_w \approx 0.5$, $b/R_b \approx 0.8$. We note here that the wing span may be smaller than the body diameter due to the location of the wing.

In Figure 11, the $\Delta(W/D)$ for case 2 is shown; the general trend is quite similar to that of case 1. In Figure 12, cases 3 and 4 are shown. For these two cases, the strength factor, $s'\overline{z}$, is 33 which is about 50 times that of case 2. The aspect ratio of the wing is about six times that of case 2, although the resulting $\Delta(W/D)$ is not too much different in these two cases. This is for the reason which has been stated before, that the

contribution of the wing to the total drag is quite small. The
difference in the $\overline{D}_m = 0.383$ and $\overline{D}_m = 0.481$ is principally due
to the drag of the body. The body volume decreases while the
thickness ratio increases with decreasing buoyancy ratio. For
$\overline{D}_m = .383$, the value of the body drag at R = .2 is about 30% of
that at R = 1, while the value for $\overline{D}_m = 0.481$ is about 40%.
This fact accounts for the low values of $\Delta(W/D)$ for the
$\overline{D}_m = 0.481$ case.

The Reynolds number effect on $\Delta(W/D)$ is examined in Figure
12. It is seen that for Re_v range of .6 to 12 x 10⁷, the differ-
ence is small for practical $\overline{C}_w \geq 0.1$.

It may be of interest now to show schematically some winged-
torpedo configurations. In Figure 14, we have shown a diameter
limited torpedo ($D_m = 21"$), and an optimum fineness ratio (5.1)
torpedo both of which weigh 3000 pounds and have a forward speed
of 45 knots when they are neutrally buoyant, and when the buoyancy
ratio = 0.8 and 0.4. It is seen that even at R = 0.4, the wings
needed in both cases are quite small. The small size of the
wing panels makes the problem of retracting them when launching
considerably simpler.

B. Range.

The results of the range calculations are shown in Figures
15 through 23. The range factor, $\ell_c S/\eta$, in miles-lb fuel/horsepower-
hour is shown as a function of buoyancy ratio with the ascending

angle as a parameter. In the first four Figures (15 through 18), the fuel weight is equal to one-half of the displacement, while in the last four Figures (19 through 22) the fuel weight is equal to one-half of the total weight. Only the results for four practical $\overline{C}_w$'s are presented; they are $\overline{C}_w$ = .01, .0204, .04, .0625.

For a torpedo of specified weight, in the case in which the fuel weight equals one-half of the displacement, since the volume of the torpedo decreases as the buoyancy ratio decreases, the fuel weight decreases with the buoyancy ratio. Although it has been shown that the overall lift-drag ratio increases with decreasing buoyancy ratio, the decrease in the amount of fuel available more than compensates for the effect with a resulting range which is always less than that obtainable by the neutrally buoyant torpedo except in descending missions. As the $\overline{C}_w$ increases, the advantages of winged-torpedo over those which are neutrally buoyant becomes more pronounced.

When the fuel weight is half of the total weight (Figures 19 through 22), the winged-torpedo has longer ranges than those with neutral buoyancy except in steep ascending missions. It is noted that the vertical scales in these Figures are different so as to exhibit the graphs more clearly.

CONCLUSIONS

1. The overall lift-drag ratios of torpedoes may be improved by the use of wings for small $\overline{C}_w$'s, say less than 0.3.

HYDRONAUTICS, Incorporated

-24-

2. For $\overline{C}_w \approx 0.01$ (3000 pound torpedo at 90 knots) the winged-torpedo of .2 buoyancy ratio may give a lift-drag ratio 2.5 - 3 times of that obtainable with a neutrally buoyant torpedo.

3. The effect of limiting the body diameter is always detrimental to the lift-drag ratio obtainable.

4. Due to the small contribution of the wing to the total drag, an increase in the strength factor $s'\overline{z}$ does not materially affect the lift-drag ratio, although it permits wings of larger aspect ratio and span.

5. The Reynolds number has little effect on the improvements attainable on the lift-drag ratio.

6. Assuming that the fuel weight equals one-half of the displacement, the winged-torpedo has longer ranges than those with neutral buoyancy only in descending missions.

7. If the fuel weight equals one-half of the total weight, the winged-torpedo has longer ranges than those with neutral buoyancy except in steep ascending missions - $\theta > 30°$.

REFERENCES

1. Young, A. D., The Calculation of the Total and Skin
    Friction Drags of Bodies of Revolution at Zero Incidence,
    A.R.C. Reports and Memoranda No. 1874, April 1939.

2. Weissinger, J., Einige Ergebnisse aus der Theorie des
    Ringflügels in Inkompressibler Strömung, "Advances in
    Aeronautical Sciences", Volume 2, Pergamon Press, 1959.

3. Lawrence, H.R., and Flax, A.H., Wing-Body Interference at
    Subsonic and Supersonic Speeds - Survey and New Developments,
    Journal of Aeronautical Sciences, volume 21, No. 5, May 1954.
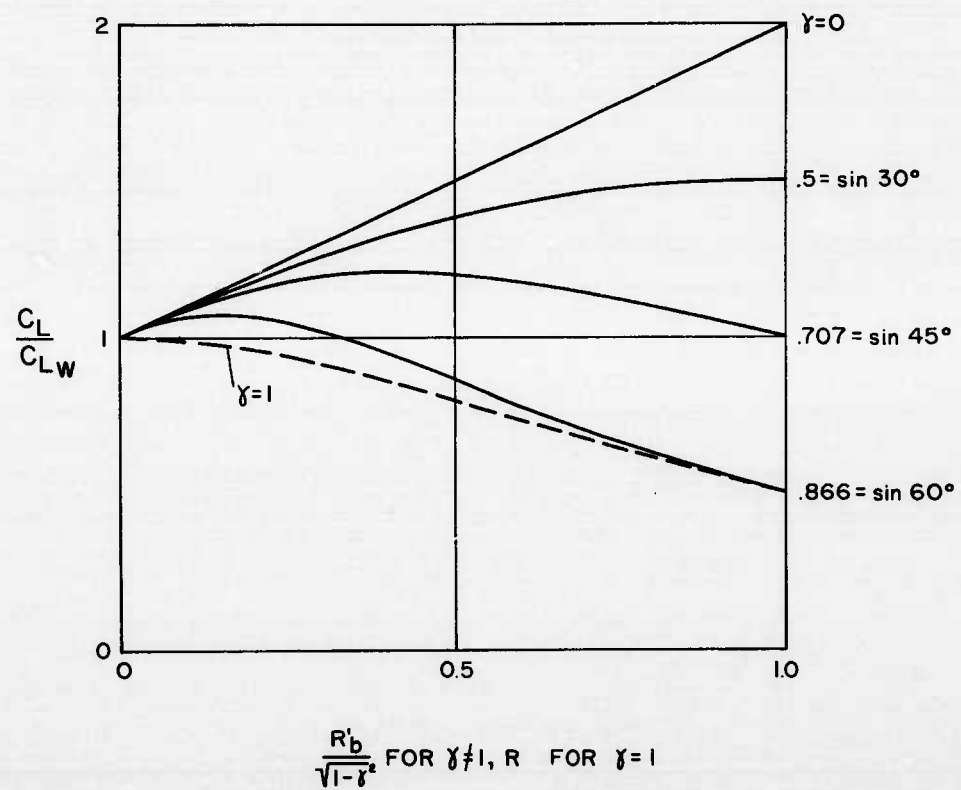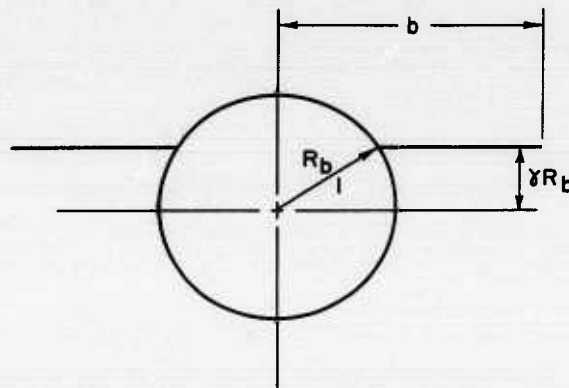
FIGURE I-EFFECT OF WING-BODY INFLUENCE ON THE TOTAL LIFT
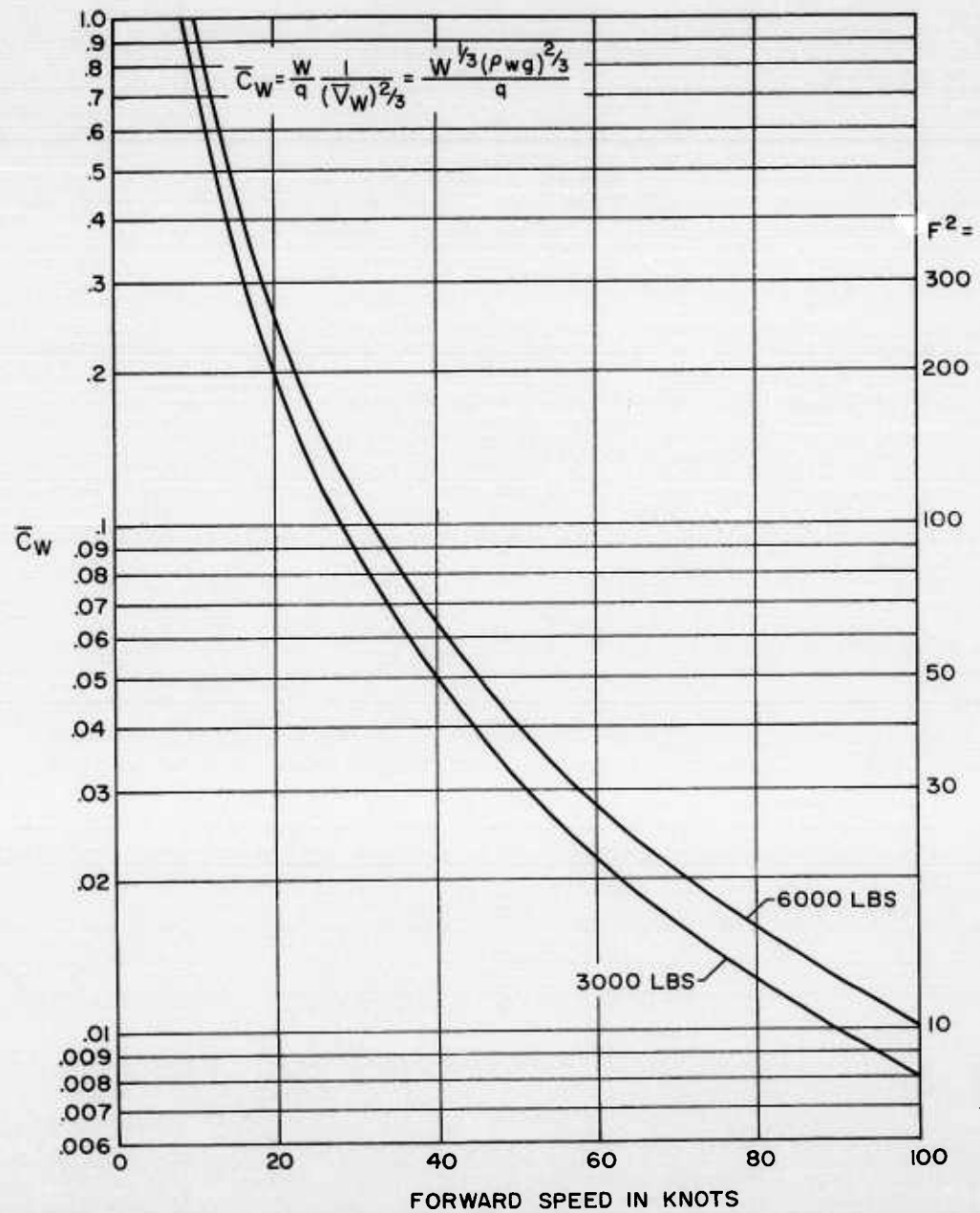
FIGURE 2-WEIGHT COEFFICIENT AS A FUNCTION OF FORWARD SPEED
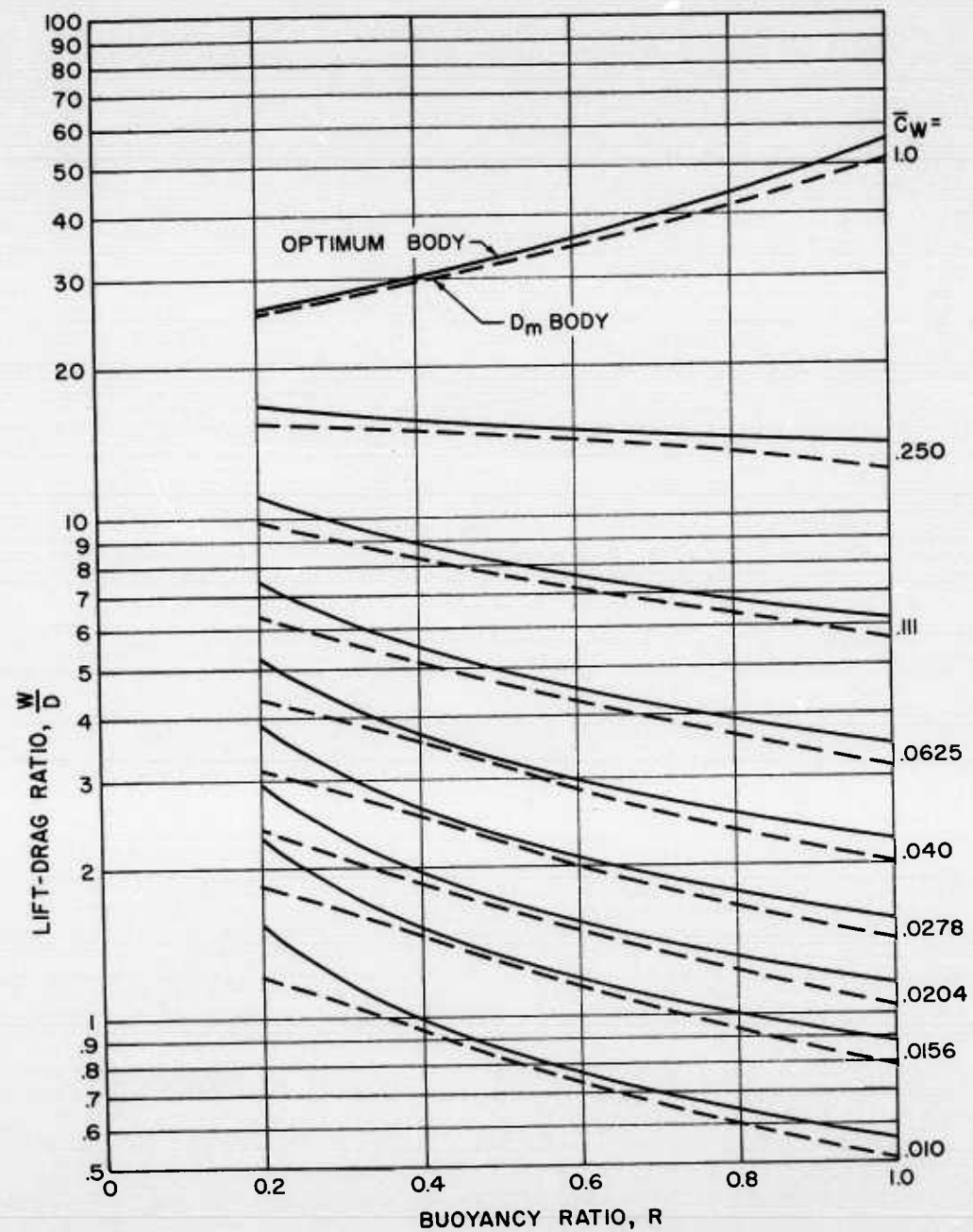
FIGURE 3-LIFT-DRAG RATIO Vs. BUOYANCY RATIO
$Rev = 12 \times 10^8$, $s\bar{z} = 0.7$, $\bar{D}_m = .481$
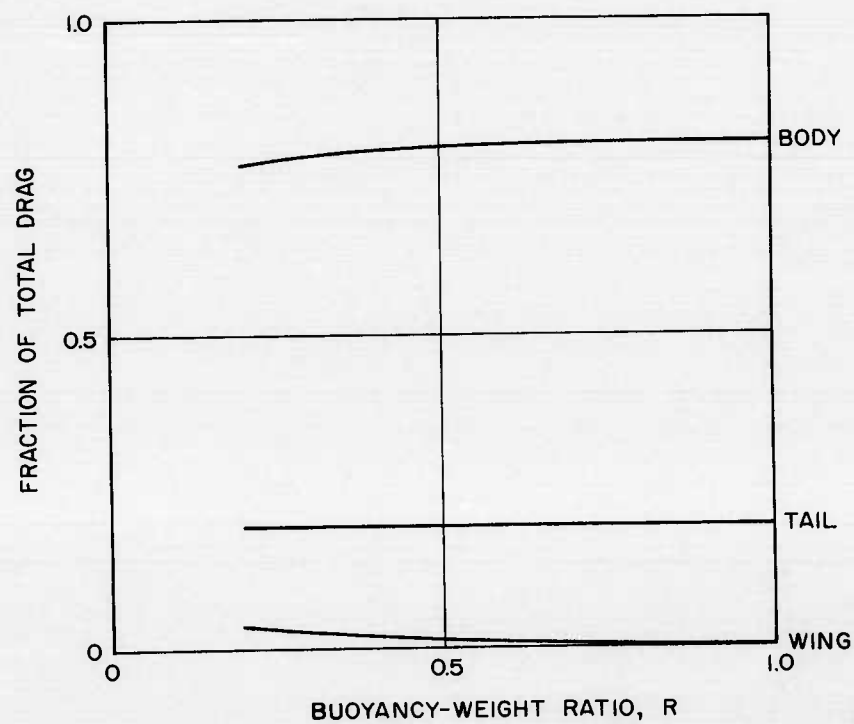
FIGURE 4-DRAG BREAK-DOWN FOR $\overline{C}_w = 0.010$
$Rev = 12 \times 10^7$, $s'\overline{z} = 0.7$ (OPTIMUM BODY)
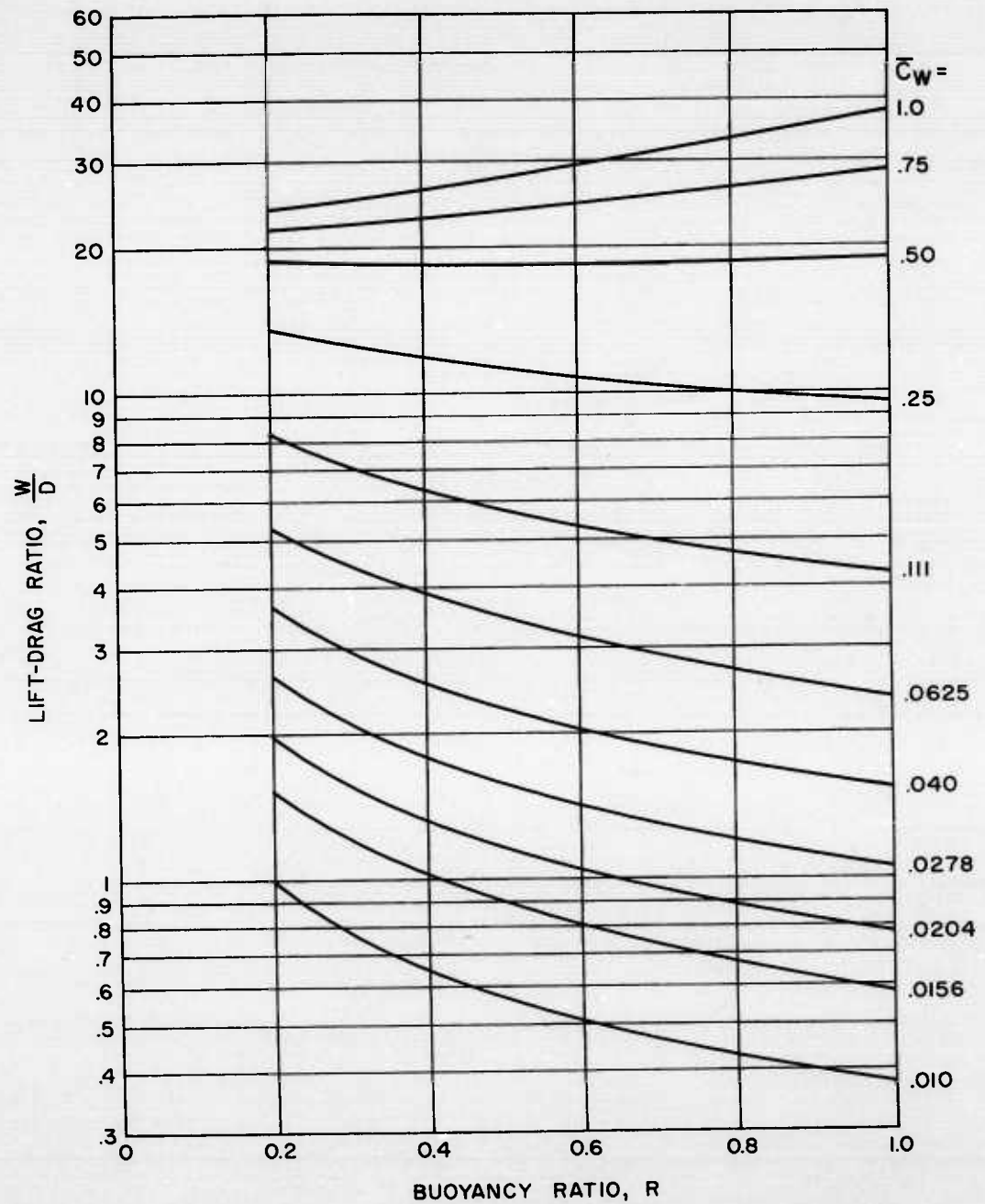
FIGURE 5-LIFT-DRAG RATIO Vs BUOYANCY RATIO. (OPTIMUM BODY ONLY)
$Rev = 6 \times 10^6$, $s'\overline{Z} = 0.7$
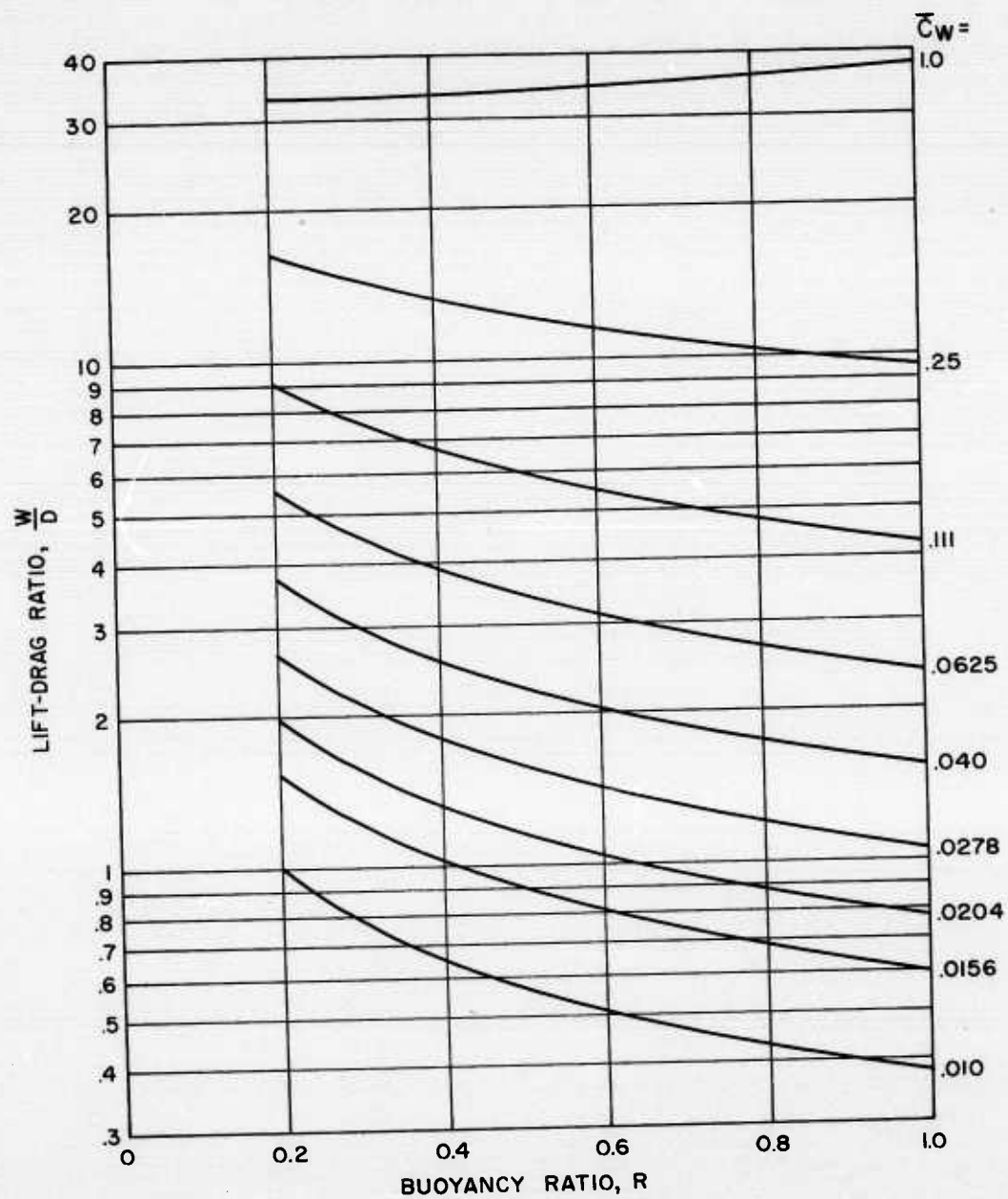
FIGURE 6-LIFT-DRAG RATIO Vs BUOYANCY RATIO
$Rev = 6 \times 10^6$, $s\bar{z} = 33$
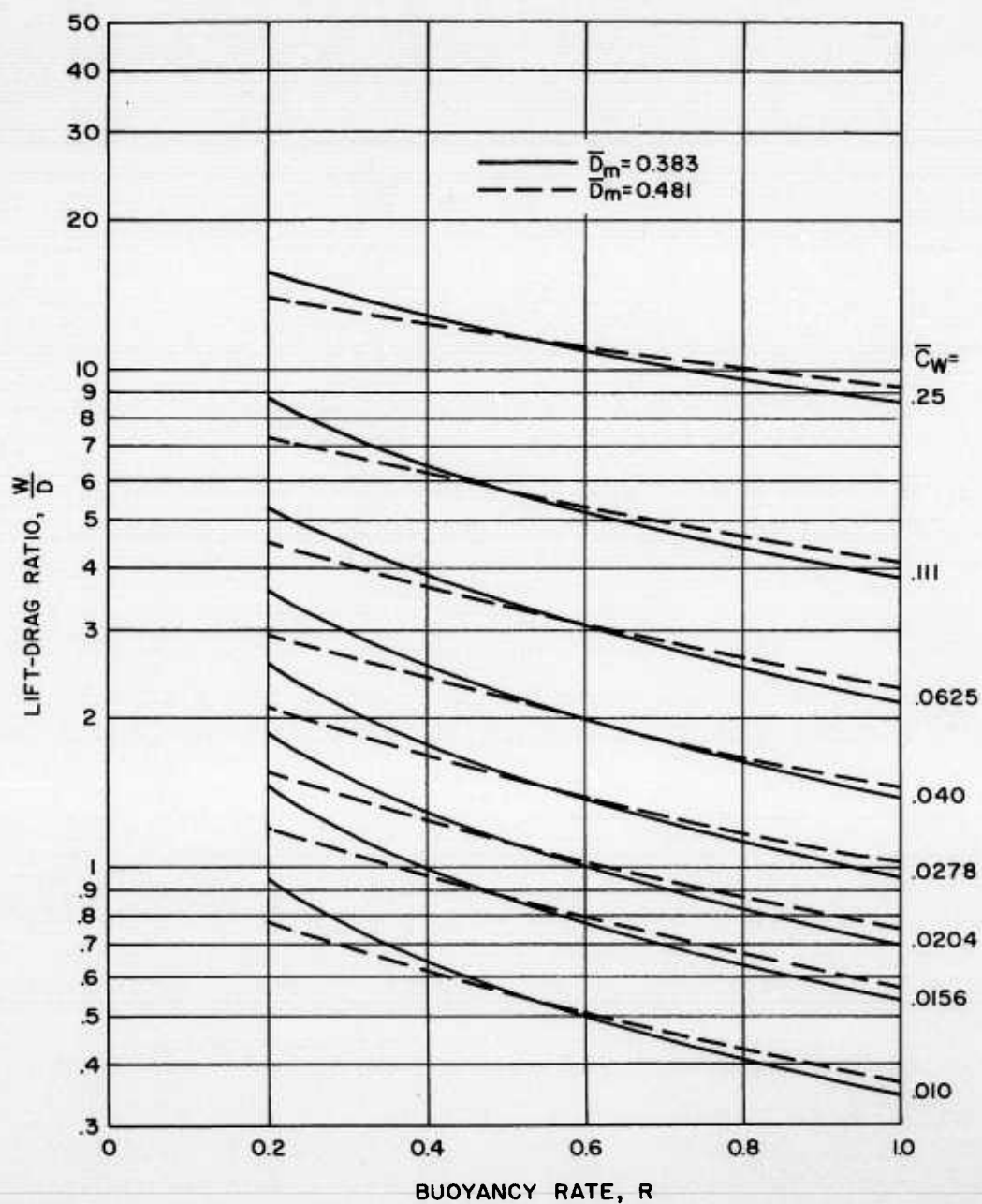
FIGURE 7-EFFECT OF $\overline{D}_m$ ON LIFT-DRAG RATIO
$Rev = 6 \times 10^6$, $s'\overline{Z} = 33$
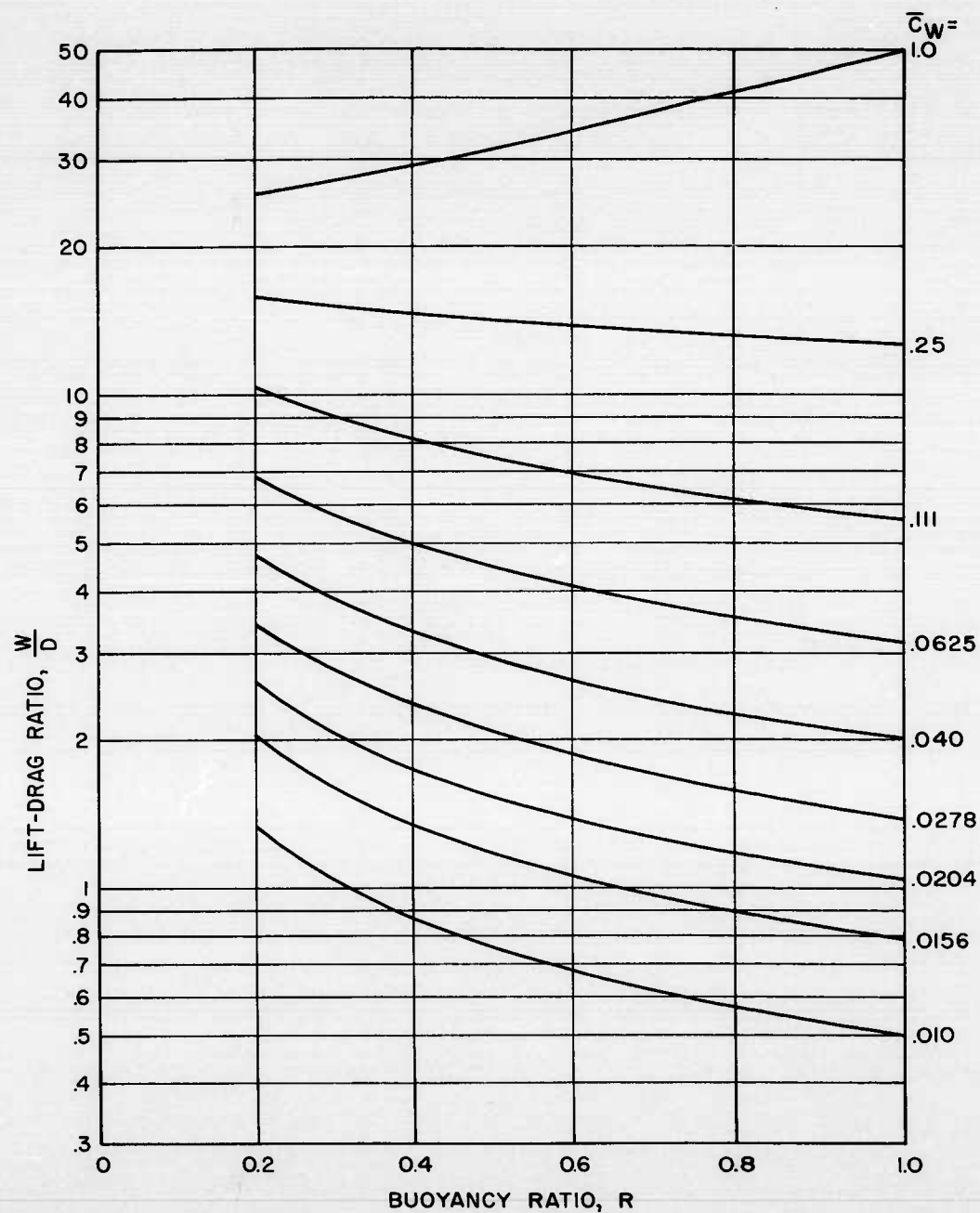
FIGURE 8-LIFT-DRAG RATIO Vs BUOYANCY RATIO

$Rev = 4 \times 10^7$, $s'\overline{z} = .7$
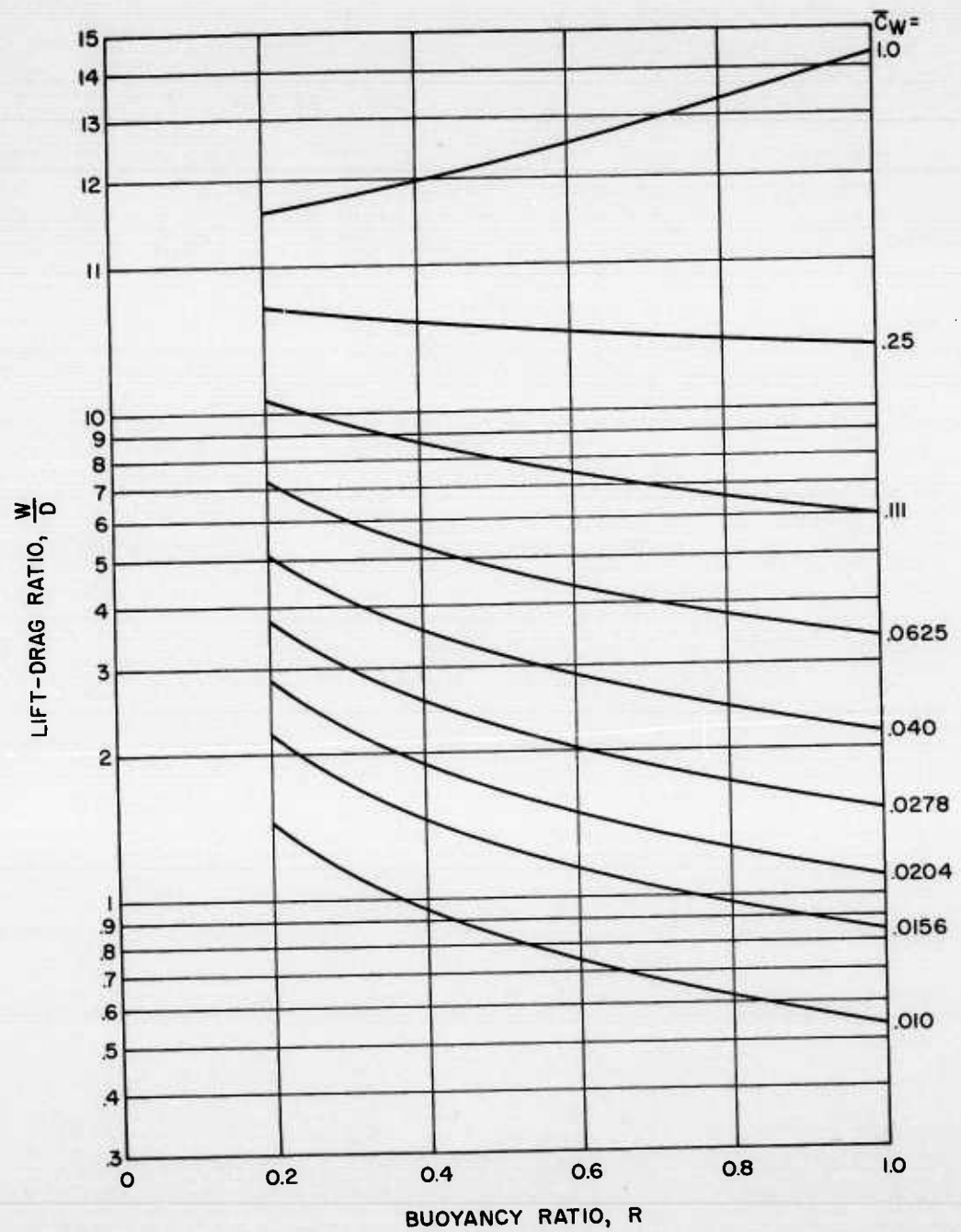
FIGURE 9-LIFT-DRAG RATIO Vs BUOYANCY RATIO
$Rev = 8 \times 10^7$, $s'\overline{z} = 0.7$
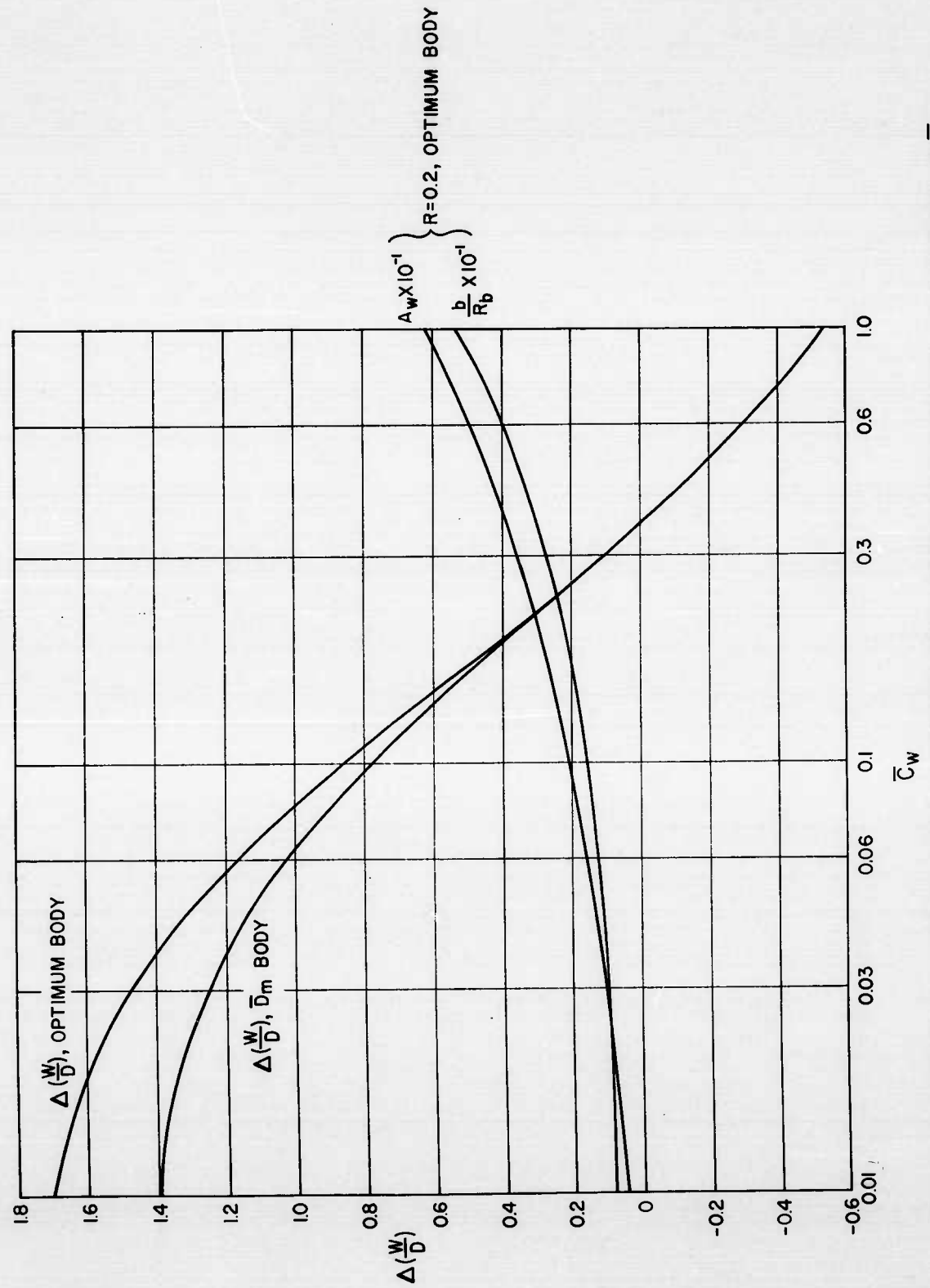
FIGURE 10-INCREASE IN LIFT-DRAG RATIO ATTAINABLE, WING ASPECT RATIO AND SPAN AS FUNCTIONS OF $\overline{C}_w$

$R_{ev} = 1.2 \times 10^8$, $s\overline{z} = 0.7$, $\overline{D}_m = 0.481$
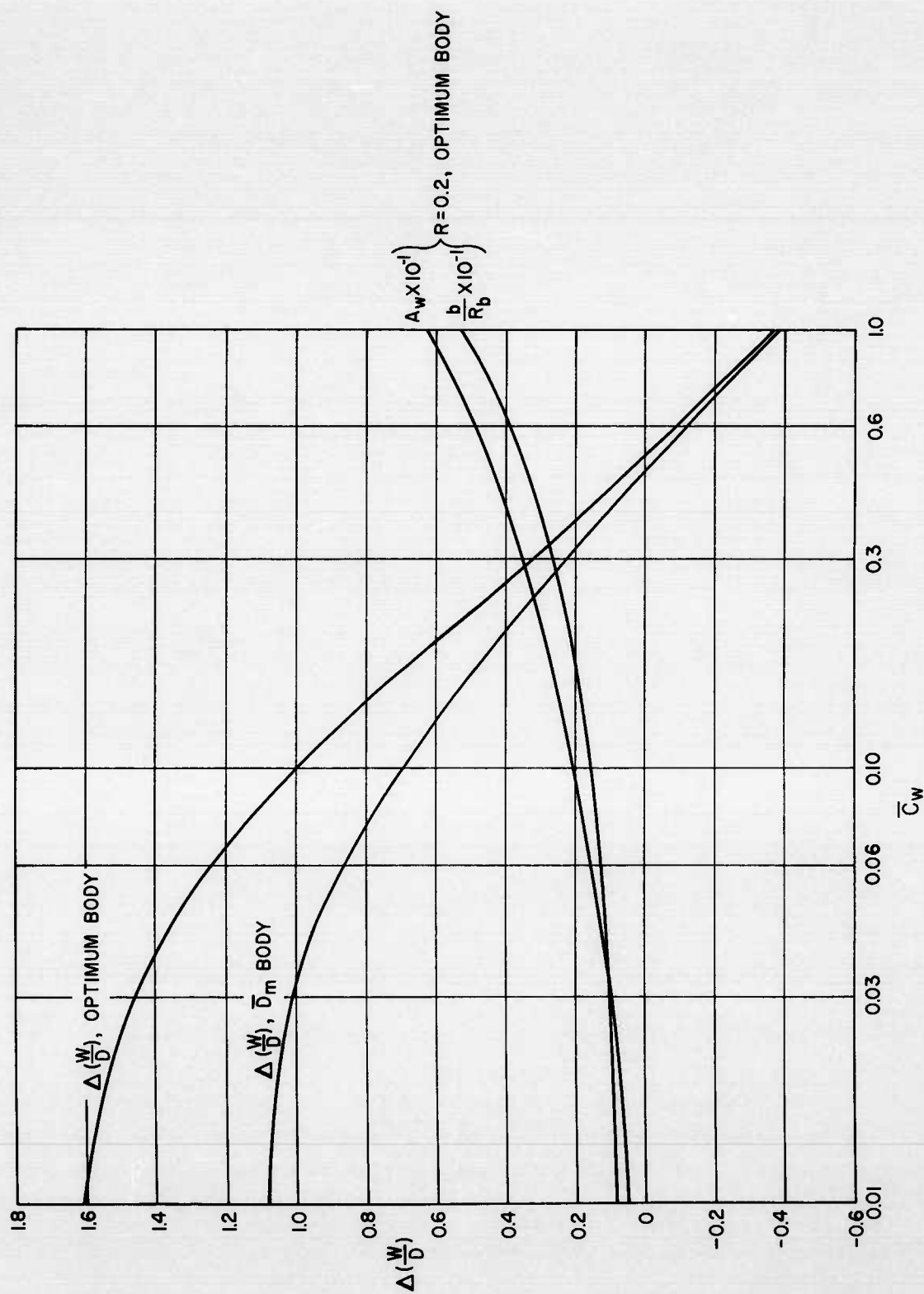
FIGURE 11-INCREASE IN LIFT-DRAG RATIO ATTAINABLE, WING ASPECT RATIO AND SPAN AS FUNCTIONS OF $\bar{C}_W$
$R_{ev} = 6 \times 10^6$, $s'\bar{z} = 0.7$, $\bar{D}_m = 0.481$
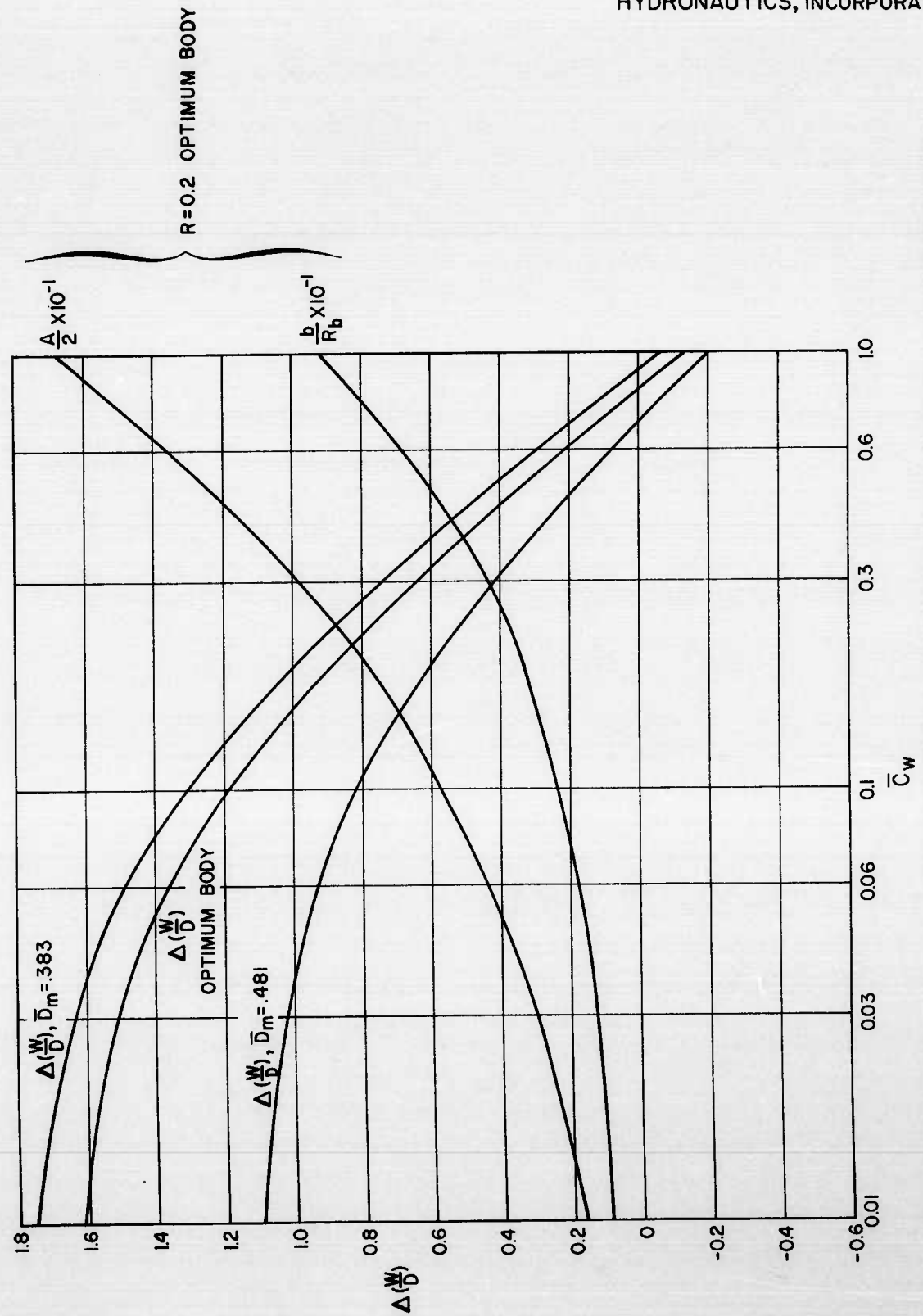
FIGURE 12-INCREASE IN LIFT-DRAG RATIO ATTAINABLE, WING ASPECT RATIO AND SPAN AS FUNCTIONS OF $\bar{C}_W$

Rev= 6X10^8, s'$\bar{Z}$=33
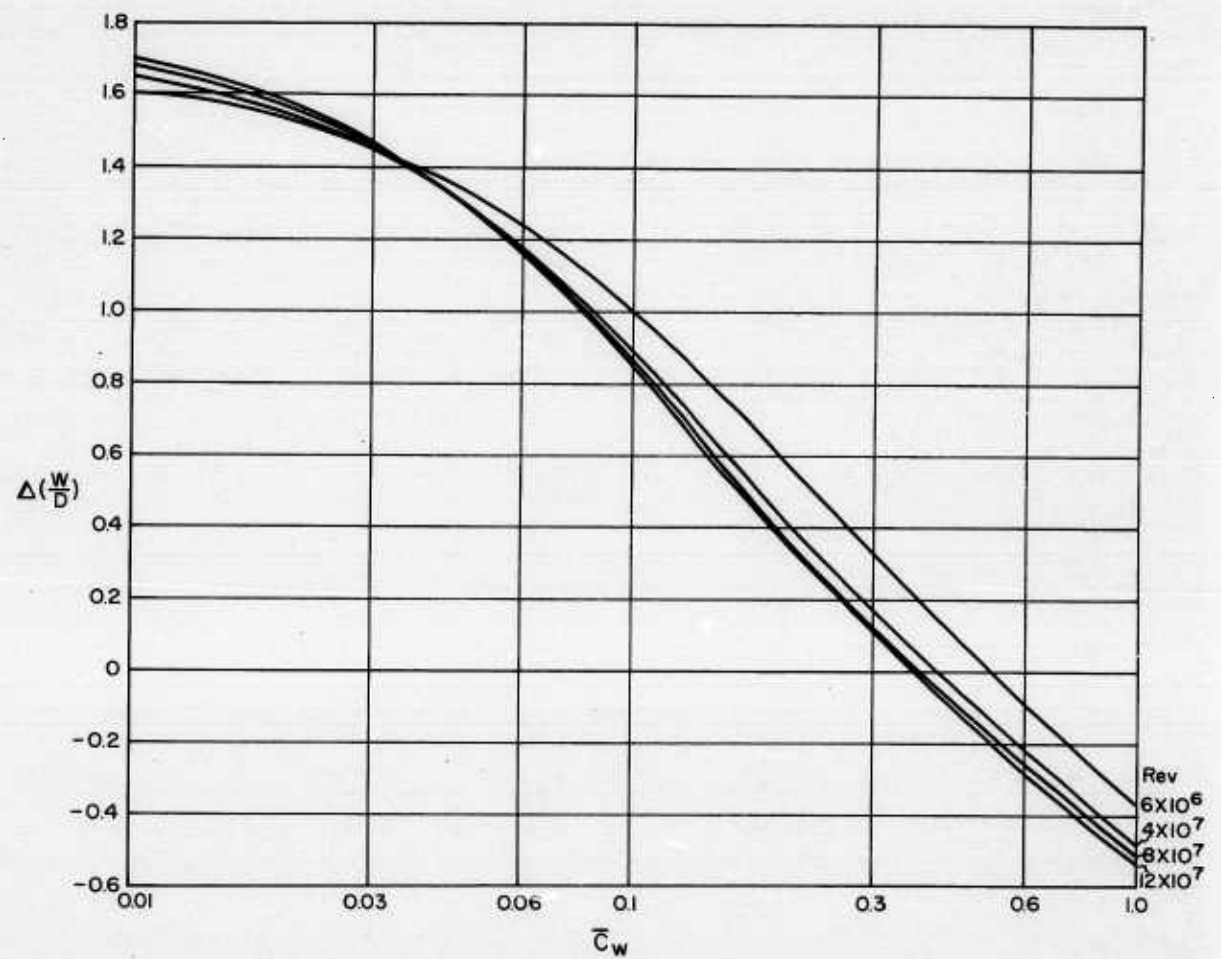
FIGURE 13-EFFECT OF Rev ON $\Delta(\frac{W}{D})$

3000 POUND, 45 KNOT TORPEDOES
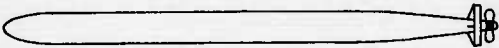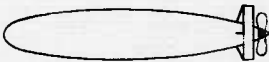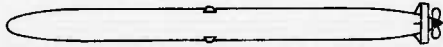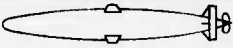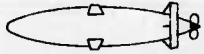
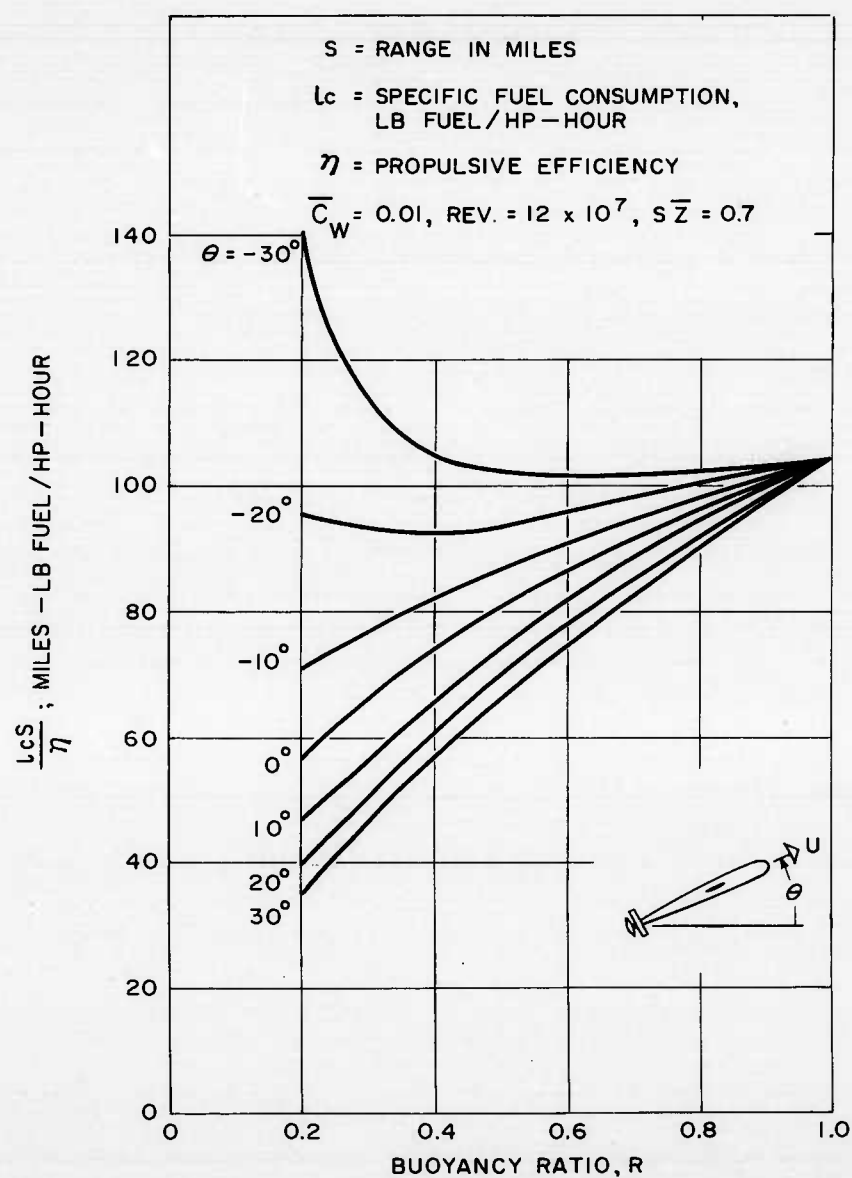| FIXED MAXIMUM DIAMETER OF 21"	OPTIMUM FINENESS RATIO OF 5
R = 1.0 D = 1490 LBS.	R = 1.0 D = 1350 LBS.
R = .8 D = 1270 LBS.	R = .8 D = 1185 LBS.
R = .4 D = 850 LBS.	R = .4 D = 810 LBS.

FIGURE 14

FIGURE 15 - THE INFLUENCE OF BUOYANCY RATIO ON RANGE
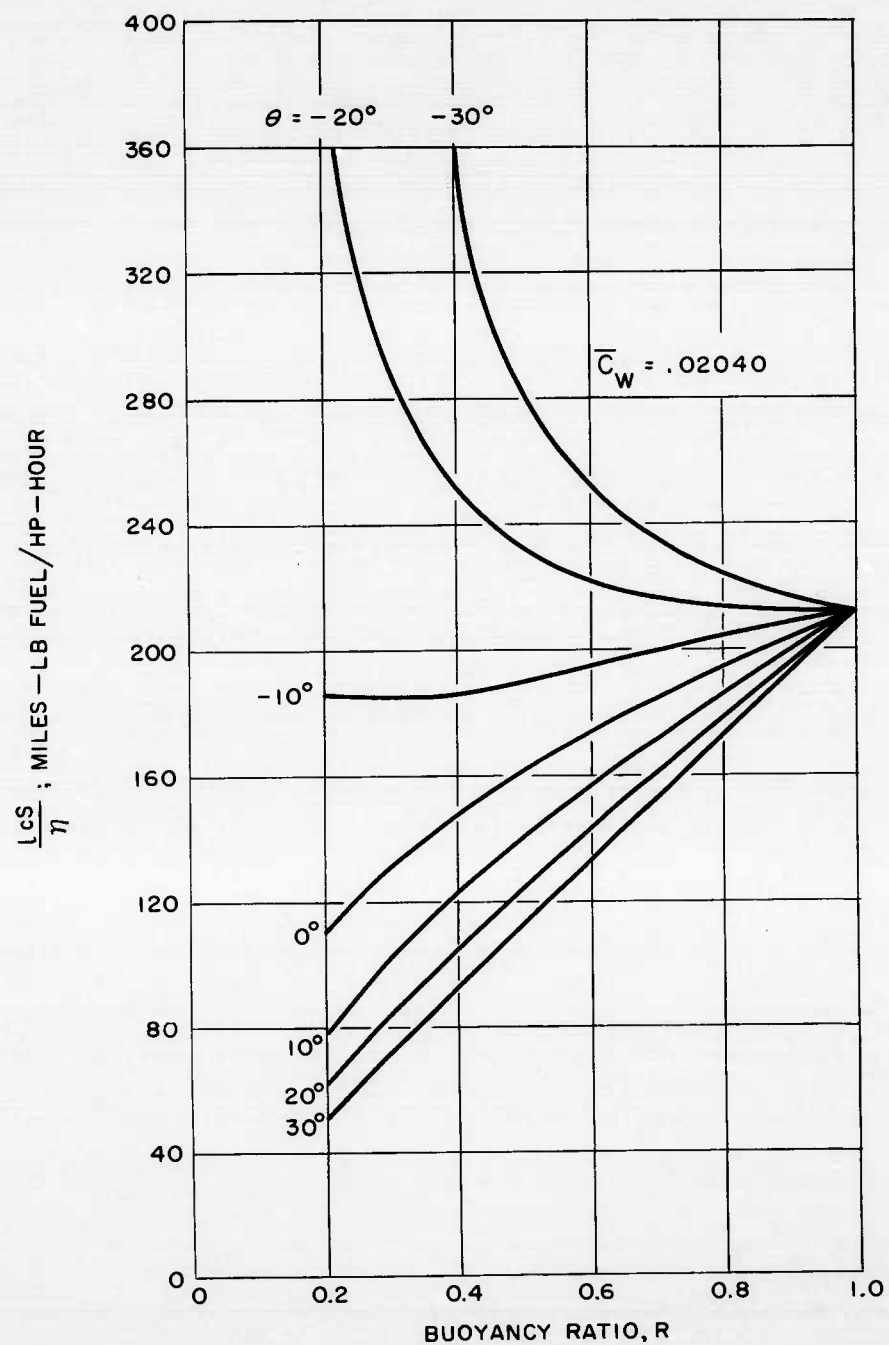(FUEL WEIGHT = .5 x DISPLACEMENT)

FIGURE 16— THE INFLUENCE OF BUOYANCY RATIO ON RANGE
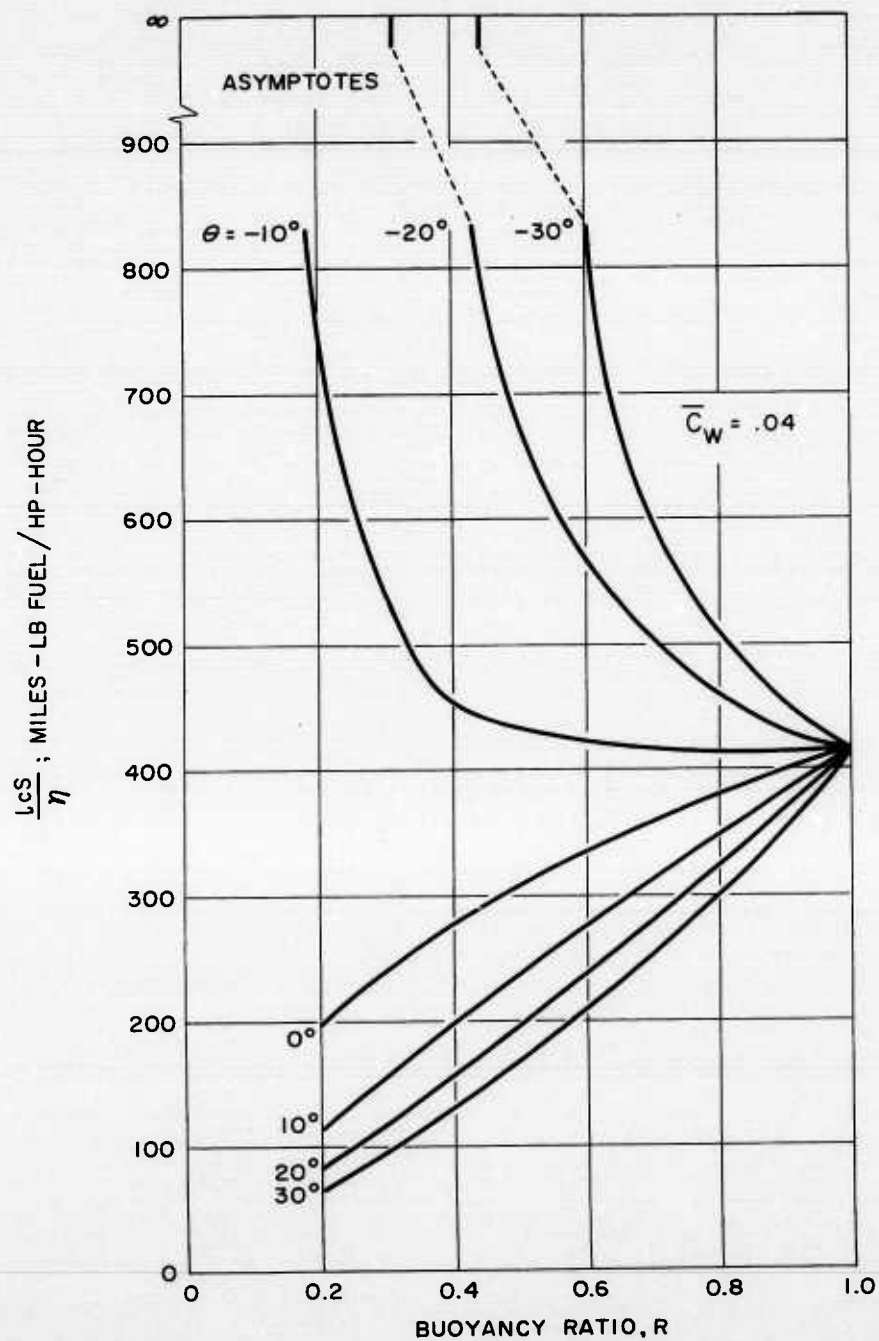(FUEL WEIGHT = .5 x DISPLACEMENT)

FIGURE 17— INFLUENCE OF BUOYANCY RATIO ON RANGE
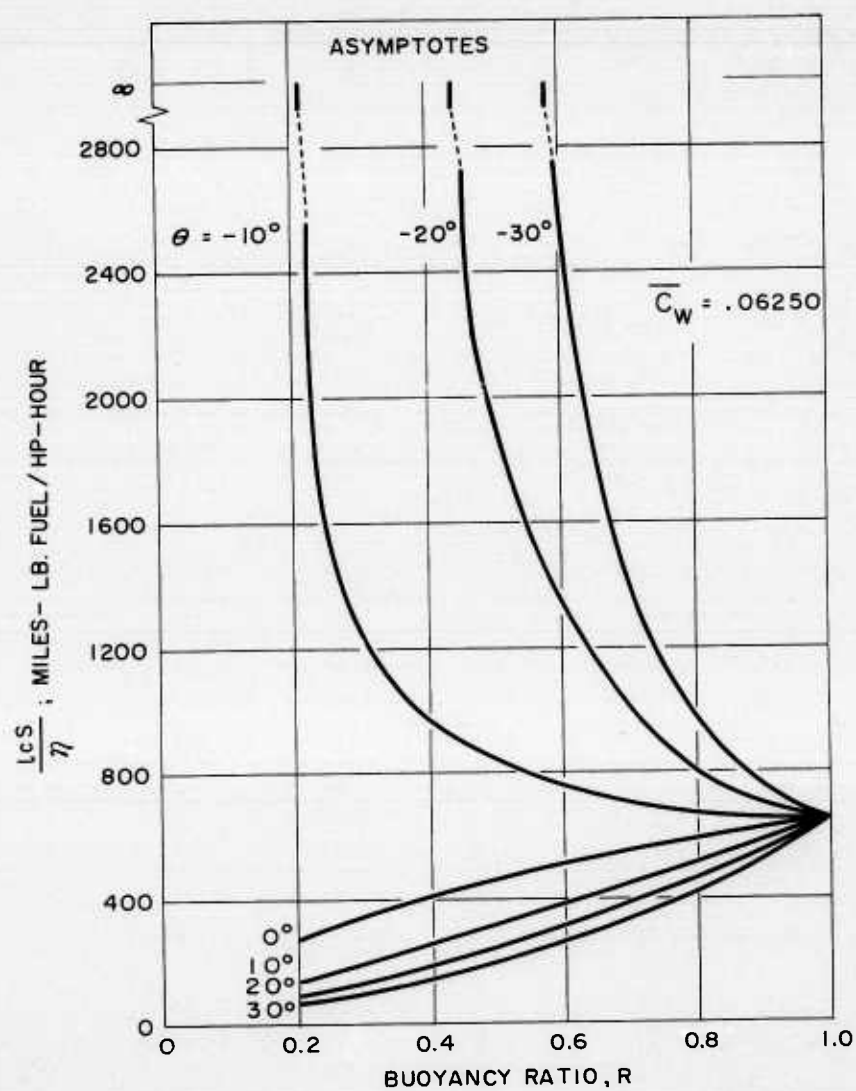(FUEL WEIGHT = .5 x DISPLACEMENT)

FIGURE 18— THE INFLUENCE OF BUOYANCY RATIO ON RANGE
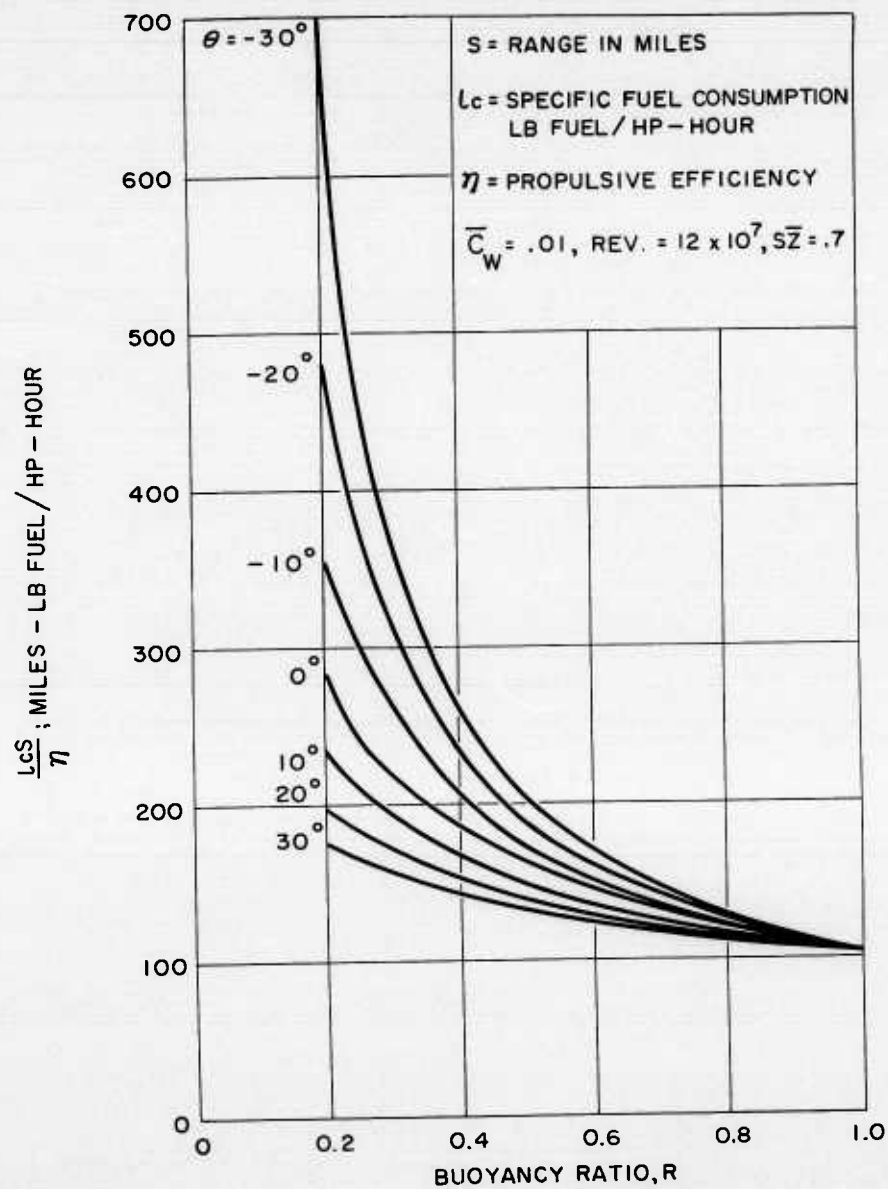(FUEL WEIGHT = .5 x DISPLACEMENT)

FIGURE 19 — THE INFLUENCE OF BUOYANCY RATIO ON RANGE
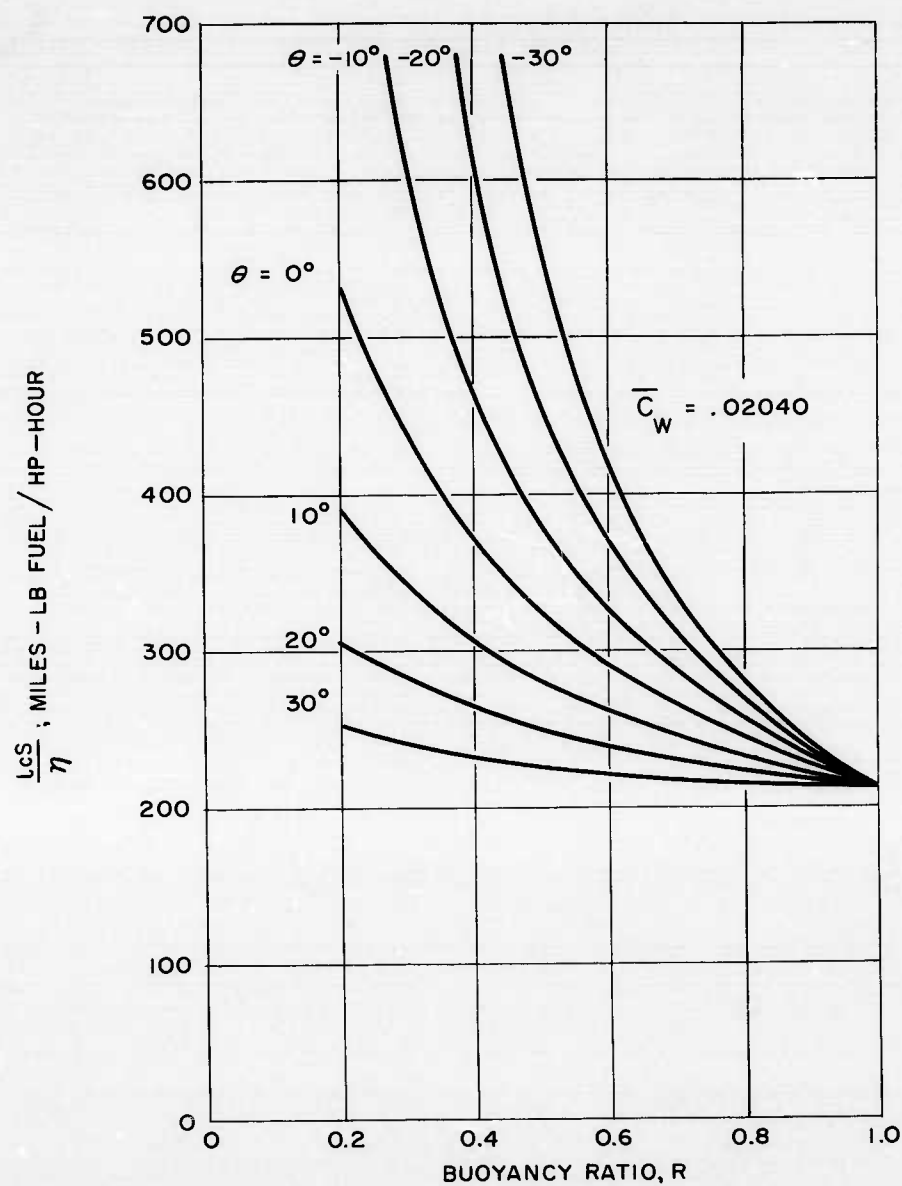
(FUEL WEIGHT = .5 W)

FIGURE 20- THE INFLUENCE OF BUOYANCY RATIO ON RANGE
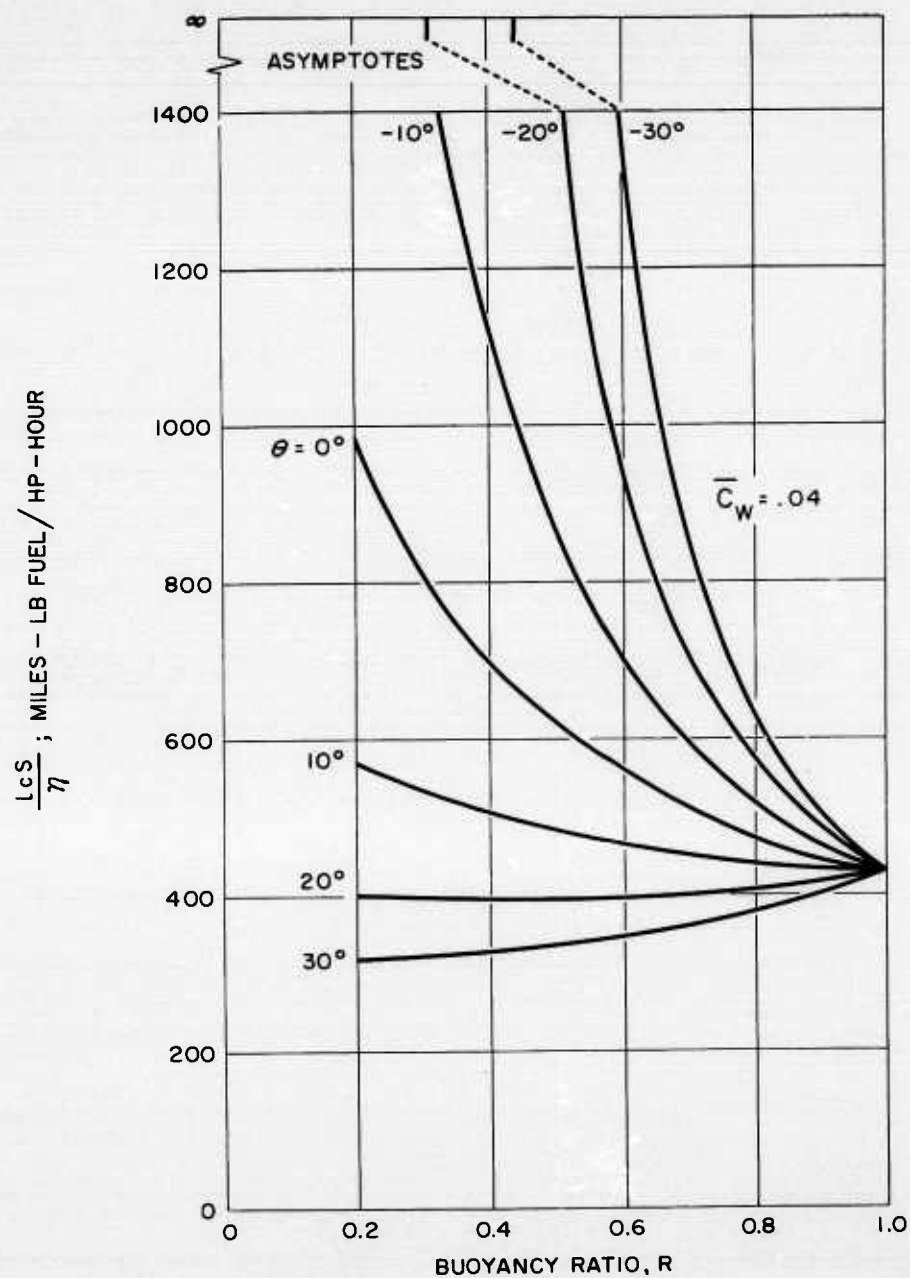(FUEL WEIGHT = .5 W)

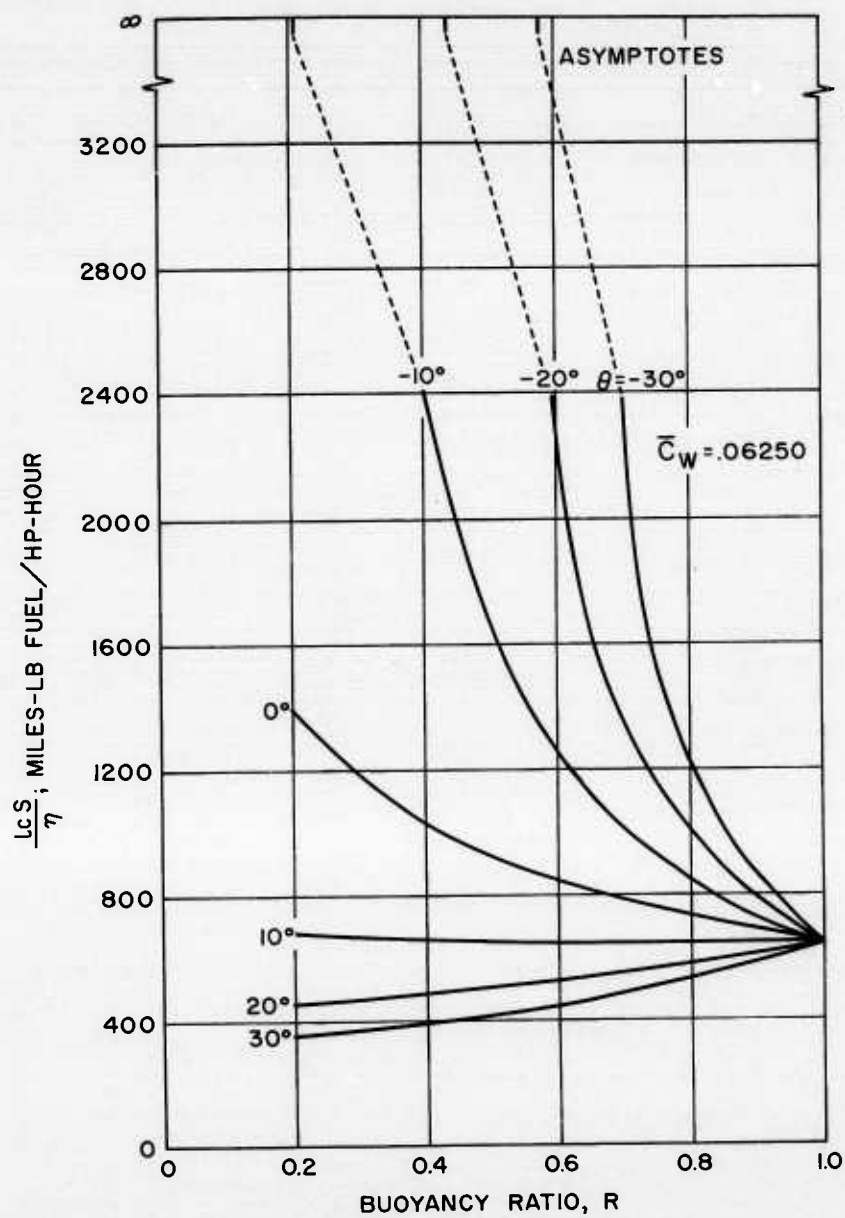FIGURE 21- THE INFLUENCE OF BUOYANCY RATIO ON RANGE
(FUEL WEIGHT = .5W)

FIGURE 22-THE INFLUENCE OF BUOYANCY RATIO ON RANGE
(FUEL WEIGHT = .5 W)

HYDRONAUTICS, Incorporated

DISTRIBUTION LIST

(Contract No. Nonr 4083(00))

Chief, Bureau of Ships (25)
Navy Department
Washington 25, D. C.
Attn: Codes 210L, 300, 300HG, 1 each
      300HM, 300HP, 300HW,   1 each
      305, 330, 340, 341B,   1 each
      342, 345, 360, 364,   1 each
      370, 373, 400, 410,   1 each
      420, 430, 436, 440,   1 each
      442, 603, 1500   1 each

U. S. Naval Research Laboratory
4555 Overlake Avenue, S. W.
Washington, D. C.
Attn: Code 2027   (6)

U. S. Naval Ordnance Test Station
China Lake, California
Attn: Code 753   1
      Pasadena Annex   1

Commanding Officer and Director (6)
David Taylor Model Basin
Washington 7, D. C.
Attn: Codes 140, 500, 530,   1 each
      550, 580, 700   1 each

U. S. Naval Ordnance Laboratory
White Oak, Maryland   1

National Academy of Sciences
National Research Council
Committee on USW,
2101 Constitution Avenue,
Washington, D. C.   1

U. S. Naval Underwater
Sound Laboratory
New London, Connecticut   1

U. S. Naval Mine Defense
Laboratory
Panama City, Florida   1

U. S. Naval Electronics
Laboratory
San Diego, California   1

U. S. Naval Air Defense Center
Johnsonville, Pennsylvania   1

U. S. Naval Underwater Ordnance
Laboratory
Newport, Rhode Island   1

U. S. Naval Ordnance Plant
Forest Park, Illinois   1

Aerojet-General Corporation
Azusa, California   1

AVCO Corporation
Wilmington,
Massachusetts   1

Clevite Ordnance
Clevite Research Center
Cleveland, Ohio   1

Secretary of Defense
Department of Defense
Washington 25, D. C.   1

HYDRONAUTICS, Incorporated

-2-

Deputy Secretary of Defense
Department of Defense
Washington 25, D. C.   1

Director of Defense Research and
Engineering
Department of Defense
Washington 25, D. C.   1

Deputy Director of Defense
Research and Engineering
(Tactical Warfare Programs)
Department of Defense
Washington 25, D.C.   1

Defense Documentation Center
for Scientific and Technical
Information
Department of Defense
Washington 25, D. C.   (30)

Assistant Secretary of the Navy
(Research and Development)
Navy Department
Washington 25, D. C.   1

Chief of Naval Operations   (9)
Navy Department
Washington 25, D. C.
Attn: Codes Op 03Eg, Op 07TC, 1 each
      Op 07T3, Op 09E,   1 each
      Op 312D, Op 322D, Op 71,1 each
      Op 91, Op 93R   1 each

Chief, Office of Naval Research (30)
Navy Department
Washington 25, D. C.
Attn: Codes 100, 102, 104,   1 each
      105, 400, 402, 402C,   1 each
      402S, 405, 406, 407,   1 each
      429, 438, 461, 463,   1 each
      466, 467, 468, 491,493 1 each
      Code 492   10

Commanding Officer
Office of Naval Research
Branch Office
Box 39, Navy No. 100,
Fleet Post Office
New York, New York   3

Commanding Officer
Office of Naval Research
Branch Office
495 Summer Street
Boston, Massachusetts 02110 (3)

Commanding Officer
Office of Naval Research
Branch Office
207 West 24th Street
New York, N. Y. 10011   3

Commanding Officer
Office of Naval Research
Branch Office
230 North Michigan Avenue,
Chicago, Illinois 60601   3

Commanding Officer
Office of Naval Research
Branch Office
1000 Geary Street
San Francisco, California 94109 (3)

Commanding Officer
Office of Naval Research
Branch Office
1030 East Green Street
Pasadena, California 91101   3

HYDRONAUTICS, Incorporated

-3-

Chief, Bureau of Naval Weapons (17) HYDRONAUTICS, Incorporated
Navy Department   Pindell School Road
Washington 25, D. C.   Howard County
Attn: Codes CU, CU-2, CU-3,   1 each Laurel, Maryland   1
      CU-4, CU-8, CPP-3,   1 each
      DLI-3, R-56, RAAD-3,   1 each
      RAAV-222, RAAV-5,   1 each
      RRE, RU, RUTO, RUTO-2, 1 each
      RUTO-3, SP-001   1 each

General Electric
Ordnance Division
Pittsfield, Massachusetts   1

Lear Siegler, Inc.
Cleveland, Ohio   1

Northrop Corporation
Hawthorne, California   1

Ordnance Research Laboratory
University Park, Pennsylvania   1

Texaco Experiments, Inc.
Richmond, Virginia   1

Thompson Ramo Wooldridge, Inc.
23555 Euclid Avenue
Cleveland 17, Ohio   1

Vitro Corporation
14000 Georgia Avenue
Silver Spring, Maryland   1

Westinghouse Electric Corporation
Ordnance Department
P. O. Box 1797
Baltimore, Maryland 21200   1